



## 저작자표시-비영리-변경금지 2.0 대한민국

이용자는 아래의 조건을 따르는 경우에 한하여 자유롭게

- 이 저작물을 복제, 배포, 전송, 전시, 공연 및 방송할 수 있습니다.

다음과 같은 조건을 따라야 합니다:



저작자표시. 귀하는 원저작자를 표시하여야 합니다.



비영리. 귀하는 이 저작물을 영리 목적으로 이용할 수 없습니다.



변경금지. 귀하는 이 저작물을 개작, 변형 또는 가공할 수 없습니다.

- 귀하는, 이 저작물의 재이용이나 배포의 경우, 이 저작물에 적용된 이용허락조건을 명확하게 나타내어야 합니다.
- 저작권자로부터 별도의 허가를 받으면 이러한 조건들은 적용되지 않습니다.

저작권법에 따른 이용자의 권리는 위의 내용에 의하여 영향을 받지 않습니다.

이것은 [이용허락규약\(Legal Code\)](#)을 이해하기 쉽게 요약한 것입니다.

[Disclaimer](#)

공학박사 학위논문

# **Performance Improvement of Inertial Navigation System Based on Frequency Domain Approaches**

주파수 영역 접근방식에 의한 관성항법시스템의  
성능향상

2014년 2월

서울대학교 대학원

기계항공공학부

강 철 우

# **Performance Improvement of Inertial Navigation System Based on Frequency Domain Approaches**

A Dissertation  
by  
Chul Woo Kang

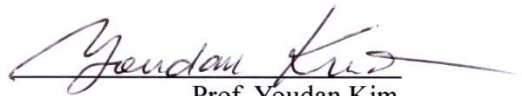
Submitted to the Department of Mechanical & Aerospace Engineering in  
partial fulfillment of the requirements for the degree of

DOCTOR OF PHILOSOPHY

in Aerospace Engineering at the

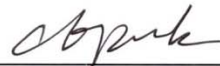
SEOUL NATIONAL UNIVERSITY  
February 2014

Approved as to style and content by:



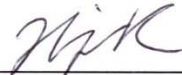
Prof. Youdan Kim

Dept. of Mechanical & Aerospace Engineering, Chairman of Committee



Prof. Chan Gook Park

Dept. of Mechanical & Aerospace Engineering, Principal Advisor



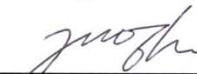
Prof. H. Jin Kim

Dept. of Mechanical & Aerospace Engineering



Prof. Hyung Keun Lee

School of Avionics and Telecommunication, Korea Aerospace University



Prof. Seong Yun Cho

Dept. of Applied Robotics, Kyungil University

# Performance Improvement of Inertial Navigation System Based on Frequency Domain Approaches

지도 교수 박 찬 국

이 논문을 공학박사 학위논문으로 제출함  
2014 년 2 월

서울대학교 대학원  
기계항공공학부  
강 철 우

강철우의 박사 학위논문을 인준함  
2014 년 2 월

위 원 장 \_\_\_\_\_ 김 유 단



부위원장 \_\_\_\_\_ 박 찬 국



위 원 \_\_\_\_\_ 김 현 진



위 원 \_\_\_\_\_ 이 형 근



위 원 \_\_\_\_\_ 조 성 윤



## **Abstract**

# **Performance Improvement of Inertial Navigation System Based on Frequency Domain Approaches**

Chul Woo Kang

Mechanical and Aerospace Engineering

The Graduate School

Seoul National University

In this dissertation, we discuss a performance improvement method in which frequency domain approaches are applied to an inertial navigation system. The conventional inertial navigation system (INS) algorithm computes all navigation solutions in the time domain. The conventional INS has limitations in it is impossible to resolve some problems by computation in the time domain, such as the observability problem of transfer alignment and the coning/sculling error mitigation algorithm. Thus, frequency domain approaches are applied to resolve the problems.

For the first topic, the frequency domain approach is applied to the transfer alignment method. Typical transfer alignment algorithms estimate the initial attitude and velocity of a projectile using the INS result of the launcher as a measurement. Typical methods have low accuracy for a steady state launcher due to the lack of observability. Thus, a new transfer alignment algorithm using the frequency domain approach is proposed in order to solve observability problem. Amplitude measurements obtained by using a discrete

time Fourier transform are applied to transfer alignment algorithm as new measurements and these serve to augment the conventional transfer alignment filter. In simulational results, yaw estimation performance improved with a vibration signal. The proposed algorithm is superior to conventional algorithms in rapid transfer alignment of a steady state vehicle.

For the next topic, a coning/sculling error compensation algorithm is developed. Typical coning and sculling compensation algorithms mitigate the coning and sculling error by using the cross product between inertial sensor measurements. These methods have limitations when applied to vehicles with large coning and sculling errors, because they have theoretical performance limits. Thus, a new direct coning/sculling compensation algorithm is proposed. The continuous coning and sculling error can be expressed by using vibrating parameters such as frequency, amplitude, and phase differences. Our new method uses adaptive notch filtering that estimates the parameters in sinusoidal signals on gyro outputs. If there are continuous sinusoidal signals on gyros, an adaptive notch filter can be used to estimate the parameters of the sinusoidal signals, and a direct coning/sculling compensation algorithm computes the attitude correction term produced by the coning/sculling signal. Our simulation results show that the proposed algorithm works appropriately.

**Keywords: Inertial Navigation System, Kalman Filter, Transfer Alignment, Integrated Navigation System, Coning/sculling error**

**Student Number: 2007-20756**

# Contents

<b>Chapter 1. Introduction .....</b>	<b>1</b>
1.1 Background and Motivation .....	1
1.2 Objective and Contribution of the Dissertation .....	2
1.3 The Structure of the Dissertation .....	7
<b>Chapter 2. Inertial Navigation System and Its Error Equation .....</b>	<b>8</b>
2.1 Introduction.....	8
2.2 Coordinate Frames .....	9
2.3 Attitude Representation and Coordinate Transform .....	13
2.4 Inertial Navigation Algorithm.....	16
2.4.1 Attitude Computation .....	18
2.4.2 Velocity and Position Update.....	20
2.4.3 Coning and Sculling Error.....	22
2.5 INS error model .....	29
2.5.1 Attitude Error Equation .....	29
2.5.1 Position and Velocity Error Equation.....	32
2.6 Alignment.....	33
2.6.1 Coarse Alignment.....	34
2.6.2 Fine Alignment.....	37
<b>Chapter 3. Transfer Alignment using Frequency Domain</b>	

<b>Approach .....</b>	<b>41</b>
3.1 Conventional Transfer Alignment Algorithms.....	43
3.2 Performance Analysis of Conventional Alignment.....	48
3.3 New Amplitude Measurement using Vibration of the Vehicle .	56
3.3.1 Simplified Attitude Error Equation for Amplitude Measurement .....	57
3.3.2 EKF based Transfer Alignment using Amplitude .....	59
3.3.3 Transfer Alignment Algorithm using Two Vibrations .....	65
3.3.4 Simulational Result .....	67
3.3 Transfer Alignment Method using Frequency Domain Approach.....	72
3.4 Simulation Results .....	76
<b>Chapter 4. Coning and Sculling Error Mitigation by Frequency Estimation .....</b>	<b>87</b>
4.1 Coning compensation .....	88
4.2 Sculling Compensation .....	89
4.3 Adaptive Notch Filtering for Signal Estimation .....	90
4.4 Direct Coning/Sculling Compensation Algorithm.....	93
4.6 Simulation results .....	95
<b>Chapter 5. Conclusion.....</b>	<b>108</b>
<b>References .....</b>	<b>111</b>



## List of Figures

Figure 1. ECI and ECEF frame .....	10
Figure 2. The navigation frame [34] .....	12
Figure 3. Euler angles and yaw-pitch-roll rotation sequence [35] .....	15
Figure 4. INS algorithm [3, 19].....	17
Figure 5. Sculling motion.....	23
Figure 6. Transfer alignment algorithm.....	44
Figure 7. Roll error of transfer alignment on stationary vehicle .....	52
Figure 8. Pitch error of transfer alignment on stationary vehicle.....	52
Figure 9. Yaw error of transfer alignment on stationary vehicle .....	53
Figure 10. Yaw error of transfer alignment under attitude maneuver .....	54
Figure 11. Yaw error of transfer alignment under long attitude maneuver.....	55
Figure 12. Yaw error of transfer alignment under acceleration maneuver .....	56
Figure 13. Proposed Alignment Structure .....	65
Figure 14. Amplitude of vibration of a car .....	68
Figure 15. Simulated signal.....	68
Figure 16. Transfer alignment result of conventional algorithm.....	69
Figure 17. Simulation results of the proposed algorithm .....	70
Figure 18. Filter structure of amplitude measurement augmented transfer alignment.....	73
Figure 19. Accelerometer measurement on the vibrating vehicle .....	78
Figure 20. Roll error result of the conventional transfer alignment for the vibrating vehicle.....	78
Figure 21. Pitch error result of the conventional transfer alignment for the vibrating vehicle.....	79
Figure 22. Yaw error result of the conventional transfer alignment for the	

vibrating vehicle .....	79
Figure 23. Roll error of the proposed algorithm .....	80
Figure 24. Pitch error of the proposed algorithm .....	81
Figure 25. Yaw error of the proposed algorithm .....	81
Figure 26. Amplitude dependency problem .....	83
Figure 27. Yaw error result of the case with different amplitudes .....	85
Figure 28. Yaw error result of transfer alignment for 7 minutes .....	85
Figure 29. Frequency response of notch filter.....	91
Figure 30. Attitude Compensation algorithm for pure coning motion .....	93
Figure 31. Velocity compensation algorithm for sculling motion .....	95
Figure 32. Attitude result for pure coning motion.....	96
Figure 33. Attitude error for pure coning motion.....	97
Figure 34. Result of 10Hz coning motion .....	99
Figure 35. Frequency estimation result (green : x-axis, blue : y-axis) .....	100
Figure 36. Attitude result for changing coning motion .....	101
Figure 37. Attitude result for Coning motion & general linear angular rate	102
Figure 38. Velocity result for pure sculling motion.....	103
Figure 39. Velocity error of D direction for pure sculling motion .....	104
Figure 40. Rate table test with HG1700 .....	105
Figure 41. Attitude result of rate table coning motion .....	106

# **Chapter 1. Introduction**

## **1.1 Background and Motivation**

The Encyclopedia Britannica states that the navigation is the science of directing a craft by determining its position, course, and distance traveled [1]. Navigation is ordinary process of all people in daily life, because everyone want to know where they are. Navigation technology has been developed from simple dead reckoning which was used by ancient Greek mariners to modern INS/ GNSS integrated navigation.

During more than 60 years, after the first invention of the inertial navigation system (INS) in the 1950s, INS has been developed as the most popular navigation method for many autonomous vehicles. Significant improvements in INS in 1960s were results of the ballistic missile programs undertaken as a result of the Cold War, since ballistic missiles needed to have high accuracy at ranges of thousands of kilometers using autonomous navigation [2]. Since INS is independent from other sources of reference navigation signals, INS is the most appropriate navigation method that can be applied to autonomous missiles.

Pure INS consists of initial alignment algorithm, attitude computation

algorithm, and velocity and position computation algorithms. Since the INS computes the navigation solutions such as attitude and position by integrating sensor signals, small sensor errors are accumulated and the navigation error diverges [3-7] with time. Thus, accurate algorithms are required in order to achieve great navigation accuracy. In particular, initial attitude estimation has a dominant effect on navigation performance.

To achieve accurate rate navigation performance, accurate sensors and exact computation algorithms are required. In this dissertation, new approaches for exact navigation algorithms using frequency domain are proposed. The conventional INS algorithms compute all navigation solutions in the time domain, and conventional INS has limitations in that it is impossible to resolve some problems by computation in the time domain, such as the observability problem of transfer alignment and coning/sculling error mitigation algorithm. Thus, frequency domain approaches are applied in order to resolve these problems.

## **1.2 Objective and Contribution of the Dissertation**

The first problem where the frequency domain approach is applied is the transfer alignment of an inertial navigation system. This is an essential

process for most guided projectile weapons like missiles or rockets. In order to obtain an accurate measurement of the projectile's initial attitude, typical projectile weapons use a transfer alignment algorithm which computes the relative attitude between the launcher and the projectile by comparing the inertial sensor data gathered by each segment.

Since the precision of the initial launch attitude is the factor which most affects navigation performance, researchers have been working for decades to develop more accurate transfer alignment methods [8-17]. In a typical launcher-projectile setup, the INSs of the launcher and the projectile are called the master INS (MINS) and slave INS (SINS). The attitude of the SINS can be estimated by comparing the outputs of the MINS and SINS. The performance of the transfer alignment depends on the movement of the vehicle because of the observability.

However, typical transfer alignment algorithms face limitations when they are applied to stationary ground vehicles because the systems are unobservable. Transfer alignment requires slight movement of the launcher to estimate the yaw angle and to overcome the lack of observability. In the case of an aircraft, additional maneuvering can easily be generated because most aircraft are free to make small movements. In the case of ship-based launchers, accelerated motion is also automatically generated by the waves of the sea.

However, the transfer alignment of ground-based launchers is not easy because most ground vehicles do not move during a launch sequence. Thus, many ground-based launchers need to perform additional movement in order to improve alignment performance. In most scenarios, though, a launch weapon is required to be able to perform an urgent and rapid transfer alignment, leaving insufficient time for the translational maneuvers needed by the MINS. Hence, a distinct transfer alignment algorithm is needed for ground vehicles that differs from that used for seafaring and airborne vehicles.

This dissertation introduces a frequency domain approach to solve this problem. The proposed method in this paper estimates the attitude error using regular vibrations caused by the running engines or power generators onboard a vehicle in a stationary state. Vibration always occurs by engines or power generators. The amplitude of oscillation is used as measurements for the new algorithm.

It is important to be able to achieve accurate computation of attitude and velocity, and for this reason, coning and sculling error compensation algorithms are an important research topic of INS algorithm development. Attitude computation algorithms in INS have been extensively studied, because they are part of the most important process in obtaining an accurate position of a moving object. In the INS, the attitude is computed by the

integration of gyro measurements. Hence, the attitude error is composed of gyro measurement errors and computation errors. The coning error due to oscillatory motion is known to be the most serious and dominant, among the computation errors [3, 18, 19].

The estimated attitude of a body depends not only on the magnitude of gyros but also on the order of rotations. If the axis of rotation changes through a multi-axis rotation, and the order of rotation is not properly tracked, the attitude error arises, and consequently, navigation performance is degraded. Hence, the coning error, which is induced by angular oscillations on two axes with different phases, can cause significant attitude error in a vehicle experiencing large dynamic motion. This error can also arise due to periodic oscillations, such as helicopter rotor vibrations or the vibration of dithering of a ring laser gyro (RLG) [20, 21].

On the other hand, the sculling error induced by the oscillation of acceleration and angular rate can cause a large error in velocity [19, 22, 23]. When the attitude of the vehicle changes continuously, a coordinate transformation of velocity cannot be exactly computed due to the computation interval of the attitude update. This causes the velocity computation error, and the sculling error is the most significant cause of the velocity error. Coning and sculling errors have duality [22], and both are called noncommutativity

errors. For these reasons, coning error mitigation methods have been introduced in many studies. In particular, the rotation vector concept was proposed by Bortz [23], where attitude algorithms have been developed to minimize the noncommutativity error under the unpredictable motion of a vehicle. Miller suggested an algorithm to optimize the attitude computation algorithm for pure coning motion [24]. Based on this work, many algorithms have been developed and analyzed to minimize the coning error caused by gyro samples over iteration intervals [26-31]. And the sculling error compensation algorithm is developed in a similar manner [22].

The aforementioned algorithms use gyro outputs to calculate higher-order correction terms. However, these algorithms have some performance limitations because they assume that the signals are represented by polynomials. These methods have limitations in vehicles with large coning and sculling errors, because they have theoretical performance limits.

To resolve these drawbacks of using conventional coning compensation algorithms, a new compensation method based on a signal processing technique is proposed in this dissertation, based on my former papers [32, 33]. We developed a direct compensation method based on a signal processing technique and show that the algorithm can also be applied to the sculling error. We employ an adaptive notch filtering algorithm to detect a sinusoidal signal



from gyro measurements, and we propose a method to accurately estimate the frequency, magnitude, and phase of the sinusoidal signal. From these parameters, we also derive higher-order compensation terms for the correction of coning/sculling errors.

### **1.3 The Structure of the Dissertation**

This dissertation consisted of 5 chapters. Here, the first chapter introduces the background and motivation of the research, and it summarizes objectives of the overall dissertation. In chapter 2, the background theory of INS and various applications of INS are explained. A brief introduction of INS will be presented including an explanation of pure navigation algorithm and alignment algorithms. In chapter 3, a new transfer alignment algorithm is presented using frequency domain analysis. In chapter 4, a new coning and sculling mitigation algorithm is proposed. Finally, in chapter 5, the summary and conclusion of the dissertation are presented.

## **Chapter 2. Inertial Navigation System and Its Error Equation**

### **2.1 Introduction**

In this chapter, basic INS algorithms are introduced.

At the end of World War II, the basic level of INS was developed to guide the early V-2 rockets. In 1950s, inertial navigation research was undertaken by many military supported labs such as Draper Laboratory at the Massachusetts Institute of Technology (MIT). In the 1960s, as the cold war intensified, a significant improvement in the INS was achieved through ballistic missile programs. A ballistic missile needs to have high accuracy at ranges of thousands of kilometers using autonomous navigation. By “autonomous,” it is meant that no man-made signals from outside the vehicle are required to perform navigation [2]. INS performance is primarily influenced by inertial sensors, which are gyroscopes and accelerometers. Inertial sensors have been developed to different criteria. One criteria for which these sensors have been developed is to have great performance, and the other criteria is that they must be small and light. In particular, small and light inertial sensors based on MEMS have had great impact on INS

technology. Since INS technology can be applied in small devices such as cars or smartphones, a lot of new applications are emerging.

## **2.2 Coordinate Frames**

First of all, coordinate frames for the INS and attitude estimation algorithms should be defined in order to express the position and the attitude of a certain object. When the position is relatively defined by direction and distance, the coordinate frame provides the reference position and direction. The attitude of the object can be defined by the relationship between the frame representing the object and reference frame. The coordinate frames widely used in navigation applications are well explained in many text books [3, 34, 35].

### **1) Inertial Frame**

According to the Newtonian definition, the inertial frame is an ideal frame that does not rotate or accelerate [5]. This frame is important because the accelerometer and gyro measure the sensor outputs with respect to this frame. However, an ideal inertial frame is not realized in practice because the

entire universe, including galaxies and stars, is moving. Thus, a quasi-inertial frame is assumed for navigation on the Earth, and an ECI(Earth-Centered Inertial) frame is generally used. An ECI frame is fixed in space with origin at the Earth's center and with axes that are non-rotating with respect to distant stars. Its z-axis is parallel to the spin axis of the Earth and is pointing toward the North Pole. The x-axis points toward the vernal equinox, the point where the plane of the Earth's orbit about the Sun crosses the Equator going from south to north, and the y-axis completes the right hand Cartesian coordinate system. This frame is described as “i” and it is expressed in Figure 1.

## 2) ECEF Frame

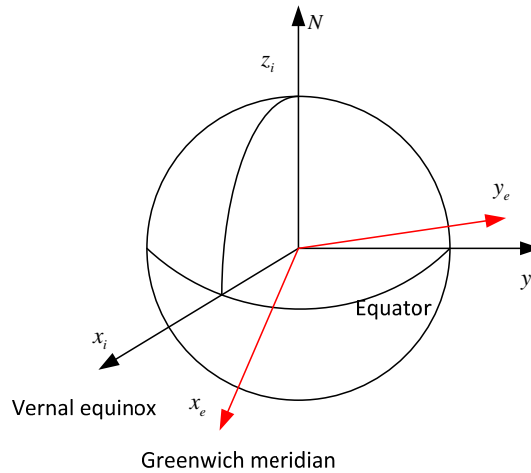


Figure 1. ECI and ECEF frame

The ECEF (Earth-Centered Earth Fixed) frame is one of the most used earth frame. It is used to define a position of a certain object on the Earth. This frame also has its origin at the Earth's center. The coordinate axes are fixed to the Earth and rotates relative to the ECI-frame with the rotation of the Earth. Due to the Earth's rotation, the ECEF frame is not an inertia reference frame. The z-axis points toward the North Pole which is same as in the ECI frame, the x-axis points toward the intersection between the Greenwich meridian and the Equator, and the y-axis completes the right handed orthogonal system. The ECEF frame is expressed as “e” and is illustrated in Figure 1.

### **3) Local Navigation Frame**

The navigation frame is a coordinate frame fixed to the Earth's surface based on the Earth surface model, such as WGS 84. It is important for computing the attitude of the body as a reference frame. The attitude of the body is defined as the differences between the navigation frame and the body frame, many navigation solutions expressed on the navigation frame, for example, ground velocity. The frame can be defined in many ways. In this

dissertation, the north-east-down (NED) system is used as a navigation frame.

The NED frame is illustrated in Figure 2.

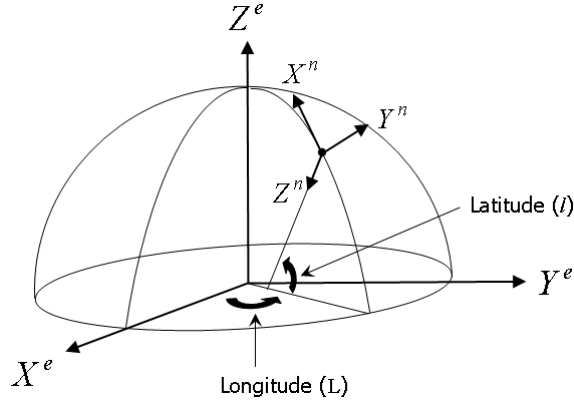


Figure 2. The navigation frame [34]

Since the navigation frame is fixed on the position of the moving body, the navigation frame rotates along the movement of the body, and the relative attitude between navigation frame and the Earth frame is defined by the geodetic latitude and longitude of the body. The transform matrix is expressed as

$$C_n^e = \begin{bmatrix} -\cos L \sin l & -\sin L & -\cos L \cos l \\ -\sin L \sin l & \cos L & -\sin L \cos l \\ \cos l & 0 & -\sin l \end{bmatrix} \quad (2.1)$$

Where,  $L$  and  $l$  represent the longitude and latitude, respectively.

#### 4) Body Frame

The body frame is defined to configure the vehicle's attitude as an orthogonal frame, and its axes are defined by engineers. In most cases of INS, the body frame is used to be defined as the sensor frame for convenience. Then, the measurements of a strapdown inertial navigation system are collected on this frame. Coinciding with the output axes of the sensor block, which is called an inertial measurement unit (IMU), the IMU raw data contains the components of the rotation rate and the acceleration experienced by a sensor unit along its body axes [5].

### 2.3 Attitude Representation and Coordinate Transform

Attitude is defined by relationships between two frames. Thus, the attitude can be expressed by a coordinate transform equation. A certain vector on “ $a$ ” is represented as  $r^a$ , and the transformation from frame  $a$  to  $b$  is defined as

$$r^b = C_a^b r^a \quad (2.2)$$

where,  $C_a^b$  is the DCM (direction cosine matrix), whose element consists of the axis direction vector of frame  $b$  observed on frame  $a$ . This DCM can be an attitude representation method. However, since the attitude has only three degrees of freedom, simpler methods are generally used [36-38].

The first attitude representation method is the famous Euler angles method. Euler angles are defined by three ordered right-handed rotations. The DCM has property of:

$$C_a^c = C_b^c C_a^b \quad (2.4)$$

Using this relationship of Euler angles, the attitude between body and navigation frame can be represented in DCM of roll  $\phi$ , pitch  $\theta$ , and yaw  $\psi$ .

$$C_b^n = C_\psi C_\theta C_\phi \quad (2.5)$$

Each DCM of roll, pitch, yaw indicate rotation through  $\phi$  about the x axis, rotation through  $\theta$  about the y axis, and rotation through  $\psi$  about the



z axis, respectively. This sequential rotation is illustrated on Figure 4, and the

Euler angles can be converted to DCM using equation (2.6)

$$C_b^n = \begin{bmatrix} \cos \theta \cos \psi & \sin \phi \sin \theta \cos \psi - \cos \phi \sin \psi & \cos \phi \sin \theta \cos \psi + \sin \phi \sin \psi \\ \cos \theta \sin \psi & \sin \phi \sin \theta \sin \psi + \cos \phi \cos \psi & \cos \phi \sin \theta \sin \psi - \sin \phi \cos \psi \\ -\sin \theta & \sin \phi \cos \theta & \cos \phi \cos \theta \end{bmatrix} \quad (2.6)$$

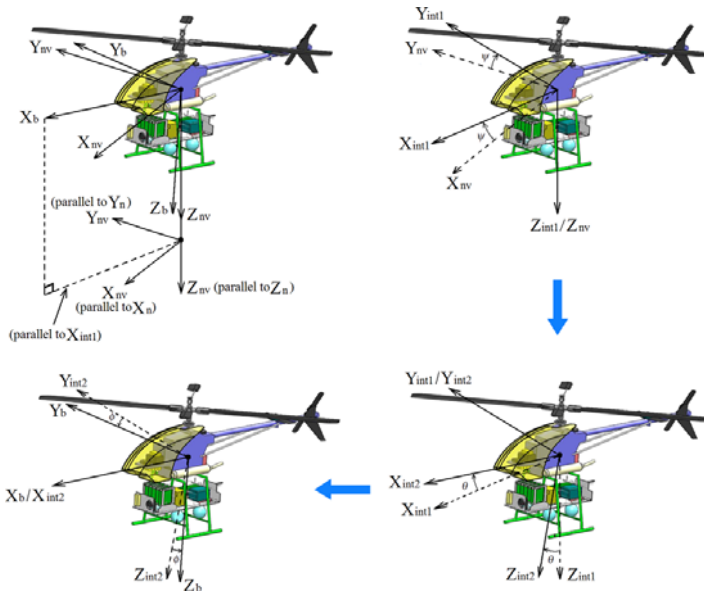


Figure 3. Euler angles and yaw-pitch-roll rotation sequence [35]

However, Euler angles can cause the singularity problem with a 90-degree pitch. Thus, the quaternions, which consist of four parameters, are

used often to avoid the singularity problem. The quaternions are expressed as

$$q = [q_0 \quad q_1 \quad q_2 \quad q_3]^T \quad (2.7)$$

With this representation, the DCM matrix can be expressed as

$$C_b^n = \begin{bmatrix} q_0^2 + q_1^2 - q_2^2 - q_3^2 & 2(q_1q_2 - q_0q_3) & 2(q_1q_3 + q_0q_2) \\ 2(q_1q_2 + q_0q_3) & q_0^2 - q_1^2 + q_2^2 - q_3^2 & 2(q_2q_3 - q_0q_1) \\ 2(q_1q_3 - q_0q_2) & 2(q_2q_3 + q_0q_1) & q_0^2 - q_1^2 - q_2^2 + q_3^2 \end{bmatrix} \quad (2.8)$$

## 2.4 Inertial Navigation Algorithm

Pure INS is used as one of the major navigation method for aerospace vehicles since its development in the 1950s. INS consists of 3-axis gyroscopes and 3-axis of accelerometers. The method by which the inertial sensors, such as the gyroscopes and accelerometers, can enable pure INS mechanization is explained in many textbooks [2-6].

The SDINS (strap down INS) provides real-time navigation solutions, such as the position, velocity, and attitude of a vehicle. These solutions are obtained by solving the fundamental equations of Newtonian classical mechanics with respect to acceleration and angular rate measurements in a

coordinate system referenced to the inertial space. To obtain acceleration and angular rate measurements, SDINS utilizes gyroscopes and accelerometers mounted directly on the vehicle. Gyroscopes provide information to compute or maintain the reference coordinate frame, and accelerometers measure specific force, which is the measurement of acceleration minus the gravity vector. For the specific force to be computed accurately, the gravity vector must be modeled properly. By separating the effects of the gravity on the accelerometers, vehicle accelerations can be precisely determined. Then SDINS integrates the acceleration twice to obtain the position without the use of external information. The main computing tasks, those of attitude determination, specific force resolution, and solution of the navigation equation, are indicated in the block diagram in Figure 4.

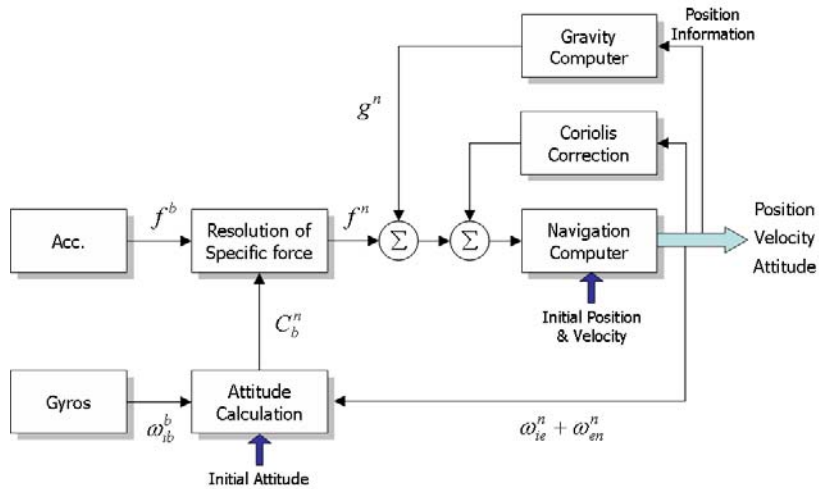


Figure 4. INS algorithm [3, 19]

### 2.4.1 Attitude Computation

The attitude update algorithm, which uses angular rate and previously known attitude, follows well known attitude kinematics equations. The attitude kinematics are differently defined by each attitude representation method.

At first, the DCM update can be done by using the following equation.

$$\dot{C}_b^n = C_b^n \Omega_{nb}^n \quad (2.9)$$

$$\Omega_{nb}^n = \begin{bmatrix} 0 & -\omega_{nb,z}^b & \omega_{nb,y}^b \\ \omega_{nb,z}^b & 0 & -\omega_{nb,x}^b \\ -\omega_{nb,y}^b & \omega_{nb,x}^b & 0 \end{bmatrix} \quad (2.10)$$

where,  $\omega_{nb}^b$  is the turn rate of the body frame with respect to the navigation frame, expressed on the body frame.  $\omega_{nb}^b$  contains  $\omega_{ib}^b$  and  $\omega_{in}^b$ .

$$\omega_{nb}^b = \omega_{ib}^b + \omega_{ni}^b = \omega_{ib}^b - C_n^b (\omega_{ie}^n + \omega_{en}^n) \quad (2.11)$$

$\omega_{ib}^b$  is the turn rate of the body frame with respect to inertial frame, it means that the angular rate is measured by gyroscopes.  $\omega_{ie}^n$  is the turn rate of

the Earth frame respect to the inertial frame, that is, the turn rate of the Earth. And  $\omega_{en}^n$  is the turn rate of the navigation frame with respect to the Earth frame, and it is called as the transport rate. The transport rate is defined by a body's velocity vector and position, and can be expressed as

$$\omega_{en}^n = \begin{bmatrix} \frac{v_E}{R_0 + h} & \frac{-v_N}{R_0 + h} & \frac{-v_E \tan L}{R_0 + h} \end{bmatrix}^T \quad (2.12)$$

where,  $R_0$  is the radius of the Earth,  $h$  is height of the body, and  $L$  is the latitude.

Using these angular rates, the DCM can be updated. However, there is a problem that arises when using the update algorithm by the DCM update. The DCM must be an orthonormal matrix, but, after updating the matrix by solving an ODE (ordinary differential equation), the solution of the ODE is not an orthogonal matrix. Thus, more simple representation methods which use smaller numbers of the parameters, for example, Euler angles or quaternions, are preferred.

The update equation for Euler angles appears as

$$\dot{\phi} = (\omega_{nb,y}^b \sin \phi + \omega_{nb,z}^b \cos \phi) \tan \theta + \omega_{nb,x}^b \quad (2.13)$$

$$\dot{\theta} = \omega_{nb,y}^b \cos \phi - \omega_{nb,z}^b \sin \phi \quad (2.14)$$

$$\dot{\psi} = (\omega_{nb,y}^b \sin \phi + \omega_{nb,z}^b \cos \phi) \sec \theta \quad (2.15)$$

These equation needs highly nonlinear computations.

On the other hand, the quaternions are updated using matrix computation.

$$\dot{\mathbf{q}} = \begin{bmatrix} q_0 & -q_1 & -q_2 & -q_3 \\ q_1 & q_0 & -q_3 & q_2 \\ q_2 & q_3 & q_0 & -q_1 \\ q_3 & -q_2 & q_1 & q_0 \end{bmatrix} \begin{bmatrix} 0 \\ \omega_{nb,x}^b \\ \omega_{nb,y}^b \\ \omega_{nb,z}^b \end{bmatrix} \quad (2.16)$$

Since the degree of freedom of the attitude is three, one constraint is needed for quaternions. The norm of quaternions must be equal to 1.

$$q_0^2 + q_1^2 + q_2^2 + q_3^2 = 1 \quad (2.17)$$

Thus, the normalization of the updated quaternion should be performed.

### 2.4.2 Velocity and Position Update

The navigation result of velocity and position in the navigation frame can

be obtained by a transformation of acceleration, which is measured on the body frame, with respect to the navigation frame.

At first, the position vector  $R$  on the ECEF frame is expressed as

$$\left. \frac{dR}{dt} \right|_i = \left. \frac{dR}{dt} \right|_e + \omega_{ie}^n \times R \quad (2.18)$$

where, the subscript of the time derivative means there is a coordinate system that performs differentiation. The acceleration on the inertial frame can be obtained by differentiating this Coriolis equation.

$$\begin{aligned} \left. \frac{dV_i}{dt} \right|_i &= \left. \frac{dV}{dt} \right|_i + \omega_{ie}^n \times \left. \frac{dR}{dt} \right|_i \\ &= \left. \frac{dV}{dt} \right|_n + (\omega_{in}^n + \omega_{ie}^n) \times V + \omega_{ie}^n \times (\omega_{ie}^n \times R) \end{aligned} \quad (2.19)$$

$$\text{where, } V_i = \left. \frac{dR}{dt} \right|_i, \quad V = \left. \frac{dR}{dt} \right|_e$$

The accelerometer measures the specific force  $f^b$ , which is expressed as a subtraction of the acceleration on the inertial frame and the mass attraction.

$$f^b = \left. \frac{dV_i}{dt} \right|_i - g \quad (2.20)$$

The mass attraction and Coriolis force constitute a local gravity vector  $g_l$  that is expressed as

$$g_l = g - \omega_{ie}^n \times (\omega_{ie}^n \times R) \quad (2.21)$$

Then, the acceleration equation can be derived from equation (2.19)

$$\dot{V}^n = C_b^n f^b - (2\omega_{ie}^n + \omega_{en}^n) \times V^n + g_l \quad (2.22)$$

where, the superscripts indicate the frame in which each vector is expressed,

and  $V^n = [V_N \ V_E \ V_D]^T$  is the velocity vector on the navigation frame.

Velocity and position on the navigation frame are computed by integration of the equation (2.22).

### 2.4.3 Coning and Sculling Error

Since the attitude is computed by the integration of a gyro measurement,



the attitude error is composed of a gyro measurement error and computation error. Among the computation error, the coning error due to oscillatory motion is known to be the most serious and dominant [3, 18-20].

The estimated attitude of a body depends not only on the magnitude of the gyros, but also on the order of rotations. If the axis of rotation changes as a result of multi-axis rotation, and the order of rotation is not properly tracked, the attitude error arises, and navigation performance is degraded consequently. Hence the coning error, which is induced by angular oscillations in two axes with different phases, can cause a significant attitude error in a vehicle experiencing a large dynamic motion. This error can also arise due to periodic oscillations such as helicopter rotor vibrations, or the vibration of a dithering of ring laser gyro (RLG) [20, 21]. The coning and sculling error must be compensated in an INS/GPS integrated navigation system [22].

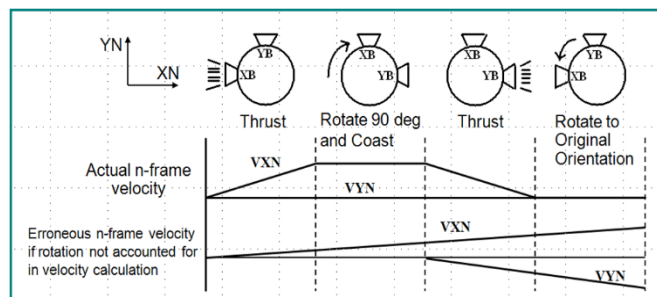


Figure 5. Sculling motion

On the other hand, the sculling error induced by the oscillation of acceleration and angular rate can cause a large error on the velocity [20, 21, 25]. When the attitude of the vehicle changes continuously, the coordinate transformation of the velocity cannot be exactly computed due to the computation interval of the attitude update. This causes the velocity computation error, and the sculling error becomes the most significant cause of velocity error. Coning and sculling errors have duality [22] and both are referred to as noncommutativity errors.

Coning errors occur due to an angular oscillation on two axes with different phases. In a coning motion, the axis of rotation is constantly changing. An axis of the system sweeps out a cone in space. For example, if there are sinusoidal signals on the X axis and Y axis with different phases, a coning error occurs on the Z axis. The angular rate of the coning motion is expressed as

$$\omega = [a\Omega \cos \Omega \tau \quad b\Omega \cos(\Omega \tau + \phi) \quad 0]^T \quad (2.23)$$

where,  $a$  and  $b$  represent the amplitude of the sinusoidal motions,  $\Omega$  is the frequency of the signal, and  $\phi$  is the phase difference of the oscillation.

An attitude update algorithm using a quaternion algorithm was derived from the following quaternion multiplication:

$$Q(t + \Delta t) = Q(t) * q(\Delta t) \quad (2.24)$$

where, \* indicates quaternion multiplication,  $Q(t)$  means quaternion on time  $t$ , and  $q(\Delta t)$  is an updating quaternion during  $\Delta t$ . The updating quaternion is expressed as

$$q(\Delta t) = [\cos(\phi_0 / 2) \quad (\phi / \phi_0) \sin(\phi_0 / 2)] \quad (2.25)$$

where,  $\phi$  represents a rotation vector and  $\phi_0$  is the norm of  $\phi$ . This rotation vector is calculated with an angular rate described by

$$\dot{\phi} = \omega + \frac{1}{2} \phi \times \omega + \frac{1}{\phi^2} \left[ 1 - \frac{\phi \sin \phi}{2(1 - \cos \phi)} \right] \phi \times \phi \times \omega \quad (2.26)$$

For practical implementation, the right-hand side of the equation (2.26) is truncated. For instance, when writing the sine and cosine terms as series

expansions and ignoring terms higher than the third order in  $\phi$ , equation (2.26) is written as

$$\dot{\phi} = \omega + \frac{1}{2}\phi \times \omega + \frac{1}{12}\phi \times (\phi \times \omega) \quad (2.27)$$

By integrating this equation, we obtain the increment angle output.

$$\phi = \alpha + \delta\phi \quad (2.28)$$

where  $\alpha$  is the increment angle, i.e., the integration of the angular rate term, and  $\delta\phi$  indicates the non-commutativity term expressed as

$$\alpha = \int_{\tau_{m-1}}^{\tau_m} \omega d\tau \quad (2.29)$$

$$\delta\phi = \frac{1}{2} \int_{\tau_{m-1}}^{\tau_m} \alpha(\tau, \tau_{m-1}) \times \omega d\tau \quad (2.30)$$

In this equation, the third order term of Eq. (2.27) is neglected. To compute  $\phi$ , we need to obtain  $\alpha$  which is a continuous function of time. But since we compute  $\alpha$  on the discrete time interval it causes the error of  $\delta\phi$  which is referred to as a non-commutativity error. Note that the coning

motion is the most severe case of the non-commutativity error.

In general coning compensation algorithms, the gyro outputs are assumed to be composed of major attitude intervals which are divided into a number of minor intervals. It is desirable to update the rotation vector for every minor interval, whereas the quaternion is updated only once in every major interval. The coning error compensation algorithms estimate the attitude error on every major interval by using a linear combination of the angle increment during the minor intervals. A generalized form of the coning integral algorithm can be written as

$$\delta\hat{\phi}_m = \left[ \sum_{j=n-p+1}^n k_{2n-j} \Delta\theta_{m-1}(j) + \sum_{j=n-p+1}^{n-1} k_{n-j} \Delta\theta_m(i) \right] \times \Delta\theta_m(n) \quad (2.31)$$

where  $n$  is the number of samples for the  $m$  th minor interval,  $p$  is the number of samples for the  $(m-1)$ -th minor interval,  $\Delta\theta_m(i)$  is the  $i$ -th gyro sample for the  $m$ -th minor interval,  $\Delta\theta_{m-1}(j)$  is the  $j$ -th gyro sample for the  $(m-1)$ -th minor interval, and  $k_{2n-j}$  and  $k_{n-i}$  are the constants for distances  $2n-j$  and  $n-i$  respectively, for  $\Delta\theta_m(n)$ .

On the other hand, sculling motion is defined as a sinusoidal angular motion on an axis with sinusoidal or linear acceleration motion on another axis, which occurs due to similar circumstances as those of coning error. Fig.1

illustrates sculling motion and its effect on gyro output. In INS, a specific force is transformed to the navigation frame to compute the navigation frame velocity. The direction cosine matrix is expressed continuously as

$$C_n^b = C_k \left[ I + \alpha \times + \frac{1}{2}(\alpha \times)^2 + \dots \right] \quad (2.32)$$

where,  $C_k$  is the direction cosine matrix of last time interval.  $\alpha$  is the angular rate term as Eq (2.7). If we denote the specific force as  $\mathbf{f}$ , the navigation frame velocity is obtained by:

$$u^n = C_k \int_{t_k}^{t_{k+1}} \left[ \mathbf{f}^b + \alpha \times \mathbf{f}^b + \frac{1}{2}(\alpha \times)^2 \mathbf{f}^b + \dots \right] dt \quad (2.33)$$

If we also define

$$v = \int_{t_k}^t \mathbf{f}^b dt \quad (2.34)$$

Then, the equation (2.33) can be rewritten as:

$$u^n = C_k \left[ v_{k+1} + \frac{1}{2} \alpha_{k+1} \times v_{k+1} + \frac{1}{2} \int_{t_k}^{t_{k+1}} (\alpha \times \mathbf{f}^b - \omega^b \times \mathbf{v}) dt \right] \quad (2.35)$$

Note that the first and second terms of right side can be computed but the third term causes some computational errors as:

$$\delta u_z^n = \frac{1}{2} \int_{t_k}^{t_{k+1}} (\alpha \times \mathbf{f}^b - \omega^b \times \mathbf{v}) dt \quad (2.36)$$

which are the cause of the sculling error. When the rotation and acceleration oscillation occur on each others axes, the non-commutativity error is generated.

## 2.5 INS error model

The INS result contains an error generated for many reasons, such as an initial alignment error, inertial sensor error, and computational error. In this section, the error model is derived to be applied to the filter model. The error equation follows the notations from the Titterton's text book[2]

### 2.5.1 Attitude Error Equation

The estimated DCM  $\tilde{C}_b^n$  contains the true DCM  $C_b^n$  and an attitude skew-symmetric error matrix  $\Psi$ .

$$\tilde{C}_b^n = [I - \Psi] C_b^n \quad (2.37)$$

$$\text{where, } \Psi = \begin{bmatrix} 0 & -\delta\gamma & \delta\beta \\ \delta\gamma & 0 & -\delta\alpha \\ -\delta\beta & \delta\alpha & 0 \end{bmatrix}$$

The elements,  $\delta\alpha$ ,  $\delta\beta$ ,  $\delta\gamma$  are the attitude errors about the x, y, and z axes, respectively. Rearranging this equation yields

$$\Psi = I - \tilde{C}_b^n C_b^{nT} \quad (2.38)$$

Differentiating this equation yields

$$\dot{\Psi} = -\dot{\tilde{C}}_b^n C_b^{nT} - \tilde{C}_b^n \dot{C}_b^{nT} \quad (2.39)$$

By definition, time differentiation of DCM is



$$\dot{C}_b^n = C_b^n \Omega_{ib}^b - \Omega_{in}^n C_b^n \quad (2.40)$$

and time differentiation of the estimated DCM can be derived in the same manner with (3.40)

$$\dot{\tilde{C}}_b^n = \tilde{C}_b^n \tilde{\Omega}_{ib}^b - \tilde{\Omega}_{in}^n \tilde{C}_b^n \quad (2.41)$$

By substituting equations (2.31) and (2.32) in equation (2.30)

$$\dot{\Psi} = -[I - \Psi] C_b^n [\tilde{\Omega}_{ib}^b - \Omega_{ib}^b] C_b^{nT} - \tilde{\Omega}_{in}^n [I - \Psi] - [I - \Psi] \Omega_{in}^n \quad (2.42)$$

Ignoring error product terms, we can get the error attitude equation of matrix.

$$\dot{\Psi} \approx \Psi \Omega_{in}^n - \Omega_{in}^n \Psi + \delta \Omega_{in}^n - C_b^n \delta \Omega_{ib}^b C_b^{nT} \quad (2.43)$$

This equation can be transformed to vector form

$$\dot{\psi} \approx -\omega_{in}^n \times \psi + \delta \omega_{in}^n - C_b^n \delta \omega_{ib}^b \quad (2.44)$$

### 2.5.1 Position and Velocity Error Equation

The differentiation of position, which is represented by latitude, longitude, and height, can be described by

$$\begin{aligned}\dot{L} &= \frac{v_N}{R_0 + h} \\ \dot{l} &= \frac{v_E}{(R_0 + h)\cos L} \\ \dot{h} &= -v_D\end{aligned}\tag{2.45}$$

By perturbation, the position error equation is derived as :

$$\begin{aligned}\delta\dot{L} &= -\frac{v_N}{(R_0 + h)^2}\delta h + \frac{1}{R_0 + h}\delta v_N \\ \delta\dot{l} &= \frac{v_E \tan L}{(R_0 + h)^2 \cos L}\delta L - \frac{v_E \sec L}{(R_0 + h)^2}\delta h + \frac{\sec L}{R_0 + h}\delta v_E \\ \delta\dot{h} &= -\delta v_D\end{aligned}\tag{2.46}$$

In this equation, Earth curvature effects are neglected.

The velocity equation can be derived from equation (2.22), and the estimated velocity is expressed as:

$$\dot{\tilde{V}}^n = \tilde{C}_b^n \tilde{f}^b - (2\tilde{\omega}_{ie}^n + \tilde{\omega}_{en}^n) \times \tilde{V}^n + \tilde{g}_l \quad (2.47)$$

The velocity error is defined by substitution of true velocity from estimated velocity. Then, the velocity error equation is

$$\begin{aligned} \delta \dot{V}^n &= \dot{\tilde{V}}^n - \dot{V}^n \\ &= \tilde{C}_b^n \tilde{f}^b - C_b^n f^b - (2\tilde{\omega}_{ie}^n + \tilde{\omega}_{en}^n) \times \tilde{V}^n - (2\omega_{ie}^n + \omega_{en}^n) \times V^n + \tilde{g}_l - g_l \end{aligned} \quad (2.48)$$

Substituting  $\tilde{C}_b^n = [I - \Psi] C_b^n$ , and writing  $\delta f^b = \tilde{f}^b - f^b$ , and neglecting the gravity vector and error product terms, we can get the following equation:

$$\delta \dot{V}^n = f^n \times \psi + C_b^n \delta f^b - (2\omega_{ie}^n + \omega_{en}^n) \times \delta V^n - (2\delta\omega_{ie}^n + \delta\omega_{en}^n) \times V^n \quad (2.49)$$

## 2.6 Alignment

Since the INS computes the attitude by integration, the initial attitude error accounts for a large proportion of the attitude error. The position error

can be affected by the initial attitude error as well. Thus, the initial attitude computation method that is the alignment has been studied due to its importance to the field of navigation.

Several methods are used as the initial alignment depending on the situation. At first, if there is no external measurement, self-alignment with contained IMU is implemented on the navigation system. Self-alignment is generally referred to alignment, which consists of two processes of coarse alignment and fine alignment. The second one is the transfer alignment, which is implemented on the INS attached to another more accurate INS. The third way of alignment is in-flight alignment, which is implemented in a system that can use external information, such as flight speed or GPS position. The in-flight alignment is not considered in this dissertation.

### **2.6.1 Coarse Alignment**

The coarse alignment is conducted in stationary vehicles on the ground. To find the attitude, which is the relation between two different frames, two vector measurements are required. In the case of a coarse alignment, the gravity vector (which is measured by accelerometers) and the Earth rotation rate (measured by gyros) are used.

Though there are many ways to compute the initial attitude, the two stage alignment method is introduced in this dissertation [5, 39]. In this method, the accelerometer measurements are used for computing the leveling attitudes, while the gyro measurements are used for estimating the heading angle.

The accelerometers measure the specific force, which is only the gravity vector on the stationary body. The measured gravity can be expressed with the following equation

$$f^b = C_n^b f^n = C_n^b [0 \quad 0 \quad -g]^T \quad (2.50)$$

where  $g$  represents the magnitude of gravity. When the vector  $f^n$  has a component in only z axis, the yaw angle is not involved in the calculation. Thus, equation (2.50) can be rewritten as:

$$f^b = \begin{bmatrix} f_x \\ f_y \\ f_z \end{bmatrix} = \begin{bmatrix} g \sin \theta \\ -g \sin \phi \cos \theta \\ -g \cos \phi \cos \theta \end{bmatrix} \quad (2.51)$$

From (2.51), the roll and pitch angles are calculated by

$$\phi = \tan^{-1} \left( \frac{-g \sin \phi \cos \theta}{-g \cos \phi \cos \theta} \right) = \tan^{-1} \left( \frac{f_y}{f_z} \right) \quad (2.52)$$

$$\theta = \tan^{-1} \left( \frac{g \sin \theta}{g \cos \theta} \right) = \tan^{-1} \left( \frac{f_x}{\sqrt{f_y^2 + f_z^2}} \right) \quad (2.53)$$

Equations (2.43) and (2.44) show that the roll and pitch angles are decided by using only accelerometer outputs.

The yaw angle can be computed from gyro measurements. When the earth rate is the only angular rate on the stationary body, then the measurement can be expressed with the following equation.

$$\omega^b = C_n^b \omega^n = C_n^b \begin{bmatrix} \Omega_{ie} \cos L & 0 & -\Omega_{ie} \sin L \end{bmatrix}^T \quad (2.54)$$

To calculate the yaw, roll and pitch angles are required. The transformation matrix  $C_n^b$  is divided into the matrix  $C_1$  containing the roll and pitch angles and  $C_2$  containing the yaw angle. Thus,  $C_1$  and  $C_2$  are given by

$$C_1 = \begin{bmatrix} \cos \theta & 0 & -\sin \theta \\ \sin \phi \sin \theta & \cos \phi & \sin \phi \cos \theta \\ \cos \phi \sin \theta & -\sin \phi & \cos \phi \cos \theta \end{bmatrix} \quad (2.55)$$

$$C_2 = \begin{bmatrix} \cos \psi & \sin \psi & 0 \\ -\sin \psi & \cos \psi & 0 \\ 0 & 0 & 1 \end{bmatrix} \quad (2.56)$$

Inserting (2.55) and (2.56) into (2.54) and rearranging yields the following equation:

$$\begin{bmatrix} \omega_x \cos \theta + \omega_y \sin \phi \sin \theta + \omega_z \cos \phi \sin \theta \\ \omega_y \cos \phi - \omega_z \sin \phi \\ -\omega_x \sin \theta + \omega_y \sin \phi \cos \theta + \omega_z \cos \phi \cos \theta \end{bmatrix} = \begin{bmatrix} \omega_N \cos \psi \\ -\omega_N \sin \psi \\ \omega_D \end{bmatrix} \quad (2.57)$$

From (2.57), the yaw angle is calculated by

$$\psi = \tan^{-1} \left( \frac{\omega_z \sin \phi - \omega_y \cos \phi}{\omega_x \cos \theta + \omega_y \sin \phi \sin \theta + \omega_z \cos \phi \sin \theta} \right) \quad (2.58)$$

The attitude calculated by coarse alignment contains large errors originating from the sensor error.

### 2.6.2 Fine Alignment

Fine alignment is the process of eliminating the remaining attitude after

coarse alignment. In the fine alignment stage, a Kalman filter is used to estimate the small misalignment angles between the reference frame and the true reference frame. The attitude error model and velocity error model in chapter 2.5 are used. The SDINS stationary error model is augmented with the use of sensors. The error system model in matrix form is expressed as:

$$\dot{x} = Ax(t) + w(t) \quad w(t) \sim N(0, Q) \quad (2.59)$$

where, the state is

$$x_f = [\delta V_N \quad \delta V_E \quad \psi_N \quad \psi_E \quad \psi_D \quad \nabla_x \quad \nabla_y \quad \varepsilon_x \quad \varepsilon_y \quad \varepsilon_z]^T \quad (2.60)$$

Since the down direction velocity error is not coupled to the other states and the down direction velocity is maintained at 0, it does not need to be estimated. The system matrix  $A$  is

$$A = \begin{bmatrix} F & T \\ 0_{5 \times 5} & 0_{5 \times 5} \end{bmatrix} \quad (2.61)$$

where,



$$F = \left[ \begin{array}{cc|cc} 0 & 2\Omega_D & 0 & g & 0 \\ -2\Omega_D & 0 & -g & 0 & 0 \\ \hline 0 & 0 & 0 & \Omega_D & 0 \\ 0 & 0 & -\Omega_D & 0 & \Omega_N \\ 0 & 0 & 0 & -\Omega_N & 0 \end{array} \right], \quad T_i = \left[ \begin{array}{cc|ccc} C_{11} & C_{12} & 0 & 0 & 0 \\ C_{21} & C_{22} & 0 & 0 & 0 \\ \hline 0 & 0 & C_{11} & C_{12} & C_{13} \\ 0 & 0 & C_{21} & C_{22} & C_{23} \\ 0 & 0 & C_{31} & C_{32} & C_{33} \end{array} \right]$$

$\delta V_N$  and  $\delta V_E$  represent the north and east velocity error.  $\psi_N$ ,  $\psi_E$ , and  $\psi_D$  represent the north, east, and down attitude errors.

$\nabla_x$  and  $\nabla_y$  are the x and y axis accelerometer biases.  $\varepsilon_x$ ,  $\varepsilon_y$ , and  $\varepsilon_z$  represent the x, y, and z axis gyro biases.

The measured signals during the stationary alignment are the horizontal velocity errors. Therefore, the observation model can be written as follows:

$$z(t) = \begin{bmatrix} I_{2 \times 2} & 0_{2 \times 8} \end{bmatrix} \begin{bmatrix} x_f(t) \\ x_a(t) \end{bmatrix} + \begin{bmatrix} v_1(t) \\ v_2(t) \end{bmatrix} \quad (2.62)$$

In order to estimate the state vectors of the error model by using the Kalman filter, the observability analysis of the error model must be performed. Due to the rank deficiency of the observability matrix, i.e.,

$$\text{Rank} \begin{bmatrix} H & HA_i & \cdots & HA_i^9 \end{bmatrix}^T = 7$$

The system is not completely observable. Therefore, only seven states are observable (the estimation value of state is convergent by Kalman filter), and the 3 states are not observable [40]. It is interesting to study which states are not observable, and much research is conducted [41-43]. The unobservable states are suggested as  $\nabla_y$ ,  $\varepsilon_y$ , and  $\varepsilon_z$  by Bar-Itzhack [41]. However, other papers claimed other states can be observable. Since several states are coupled with other states, the unobservable state can be vary by a change of the system and by decoupling. For example, by changing the system,  $\nabla_x$  can be unobservable instead of  $\varepsilon_z$ .

## **Chapter 3. Transfer Alignment using Frequency Domain Approach**

The transfer alignment of an inertial navigation system is an essential process for most guided projectile weapons such as missiles or rockets. In order to obtain an accurate measurement of the projectile's initial attitude, typical projectile weapons use a transfer alignment algorithm which computes the relative attitude between the launcher and the projectile by comparing the inertial sensor data gathered by each segment.

Since the precision of the initial launch attitude is the factor that affects navigation performance the most, researchers have been working for decades to develop more accurate transfer alignment methods [8-17]. In a typical launcher-projectile setup, the INSs of the launcher and the projectile are called the master INS (MINS) and slave INS (SINS), respectively. The attitude of the SINS can be estimated by comparing the outputs of the MINS and SINS. Browne [8] proposed a means of velocity and attitude matching between the MINS and SINS, and most research papers have used this method. Kain [9] proposed an attitude measurement formulation using the direction cosine matrix and analyzed alignment performances during several different

maneuvers. Several later studies [10-17] developed similar alignment methods for many applications, and these algorithms are well summarized in [11, 17]. Other recent studies have concentrated on the delay of measurements [13] of the flexure effect [15]. Two objectives have been emphasized in most of these works. The first objective is to achieve a shorter time for alignment, and the second one is to improve accuracy of the alignment. Those objectives are deeply related to observability. For example, an improvement of observability makes the filter converge quickly and with higher accuracy. That is, rapid alignment can be achieved.

The typical Kalman filter algorithm used in transfer alignment will be described in section 3.1. Typical transfer alignment algorithms face limitations when it comes to applications for stationary ground vehicles since the systems are unobservable. Transfer alignment requires slight movement of the launcher to estimate the yaw angle and overcome the lack of observability. In the case of an aircraft, additional maneuvering can easily be generated because most aircraft are free to make small movements. In the case of ship-based launchers, accelerated motion is also automatically generated by the waves of the sea. However, the transfer alignment of ground-based launchers is not easy because most ground vehicles do not move during a launch sequence. Thus, many ground-based launchers need to perform additional

movements in order to improve alignment performance. In most scenarios, though, the launch weapons are required to have urgent and rapid transfer alignment, leaving insufficient time for the translational maneuvers needed by the MINS. Hence, a distinct alignment algorithm for ground vehicles is needed that differs from those used for seafaring and airborne vehicles.

In this chapter, a new transfer alignment algorithm that uses frequency analysis is proposed, motivated by Soloviev's paper [44]. Soloviev and Graas proposed a frequency domain approach for sensor calibration in their study. The method proposed in this paper estimates the attitude error using regular vibrations caused by running engines or power generators onboard the vehicle that is in a stationary state. Vibration always occurs as a result of the activation of engines or power generators. The amplitude of oscillation is used as a measurements for the new algorithm.

### **3.1 Conventional Transfer Alignment Algorithms**

Depending on the system, different algorithms are designed to fit the specific purpose of the system under consideration. In this dissertation, the velocity and DCM matching method is introduced as a typical transfer alignment algorithm. The algorithm is summarized in the following figure.

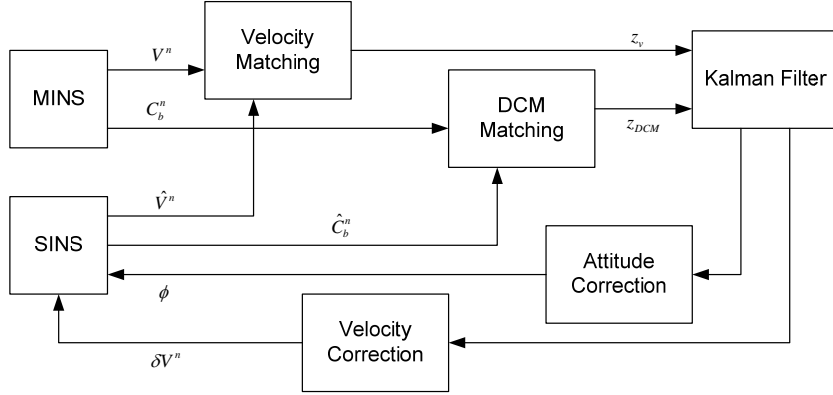


Figure 6. Transfer alignment algorithm

MINS (Master INS) represents the INS result of the launcher (submarine), and the SINS (Slave INS) means the INS result of the projectile. The state vector for the Kalman filter is composed of the velocity error  $\delta V^n$ , attitude error  $\psi$ , mis-alignment error  $\phi$ , accelerometer bias  $\nabla$ , and gyro bias  $\varepsilon$ , and can be expressed as:

$$\delta x = [\delta V^{nT} \quad \psi^T \quad \phi^T \quad \nabla^T \quad \varepsilon^T]^T \quad (3.1)$$

The process model is

$$\delta \dot{x} = F \delta x + w \quad (3.2)$$

$$\text{where, } F = \begin{bmatrix} F_{11} & F_{12} & 0_{3 \times 3} & F_{14} & 0_{3 \times 3} \\ F_{21} & F_{22} & 0_{3 \times 3} & 0_{3 \times 3} & F_{25} \\ 0_{3 \times 3} & 0_{3 \times 3} & 0_{3 \times 3} & 0_{3 \times 3} & 0_{3 \times 3} \\ 0_{3 \times 3} & 0_{3 \times 3} & 0_{3 \times 3} & 0_{3 \times 3} & 0_{3 \times 3} \\ 0_{3 \times 3} & 0_{3 \times 3} & 0_{3 \times 3} & 0_{3 \times 3} & 0_{3 \times 3} \end{bmatrix},$$

$$F_{11} = \begin{bmatrix} \frac{V_D}{R+h} & 2\Omega_D + 2\rho_D & -\rho_E \\ -2\Omega_D - \rho_D & \frac{V_D}{R+h} & 2\Omega_N + \rho_N \\ 2\rho_E & -2\Omega_N - 2\rho_N & 0 \end{bmatrix}, \quad \begin{matrix} F_{12} = f^n \times \\ F_{14} = C_b^n \end{matrix},$$

$$F_{21} = \begin{bmatrix} 0 & \frac{1}{R+h} & 0 \\ \frac{-1}{R+h} & 0 & 0 \\ 0 & \frac{-\tan L}{R+h} & 0 \end{bmatrix}, \quad \begin{matrix} F_{22} = \begin{bmatrix} 0 & \Omega_D + \rho_D & -\rho_E \\ -\Omega_D - \rho_D & 0 & \Omega_N + \rho_N \\ \rho_E & -\Omega_N - \rho_N & 0 \end{bmatrix}, \\ F_{25} = -C_b^n \end{matrix}$$

The measurements are the difference of the velocity and the difference of the DCM between the MINS and SINS. When the MINS is assumed to be perfect, the differences are considered to be the error of the SINS. The velocity error is :

$$z_v = \bar{V}^{n,M} - \hat{V}^{n,M} = V^{n,M} - \hat{V}^{n,M} + v_v \quad (3.3)$$

where,  $V^{n,M}$  is the true velocity of MINS,  $\bar{V}^{n,M}$  is the measured velocity of MINS,  $\hat{V}^{n,M}$  is the estimated velocity of the MINS by estimated using the SINS velocity, and  $v_v$  is the Gaussian noise of the velocity of the MINS.

In this case, the lever arm effect must be considered. The lever arm effect is the velocity components of the SINS which is caused by the angular motion of the master. The lever arm velocity is expressed as:

$$\begin{aligned} V^{n,M} &= V^{n,S} - \left. \frac{dL}{dt} \right|_n \\ &= V^{n,S} - C_b^n \omega_{nb}^b \times L^b = V^{n,S} + \omega_{in}^n \times C_b^n L^b - C_b^n \omega_{ib}^b \times L^b \end{aligned} \quad (3.4)$$

where  $L^b$  is the position of the SINS relative to the MINS. Taking this effect into consideration, the velocity measurement equation can be derived as

$$z_v = V^{n,M} - \hat{V}^{n,S} - \left( \omega_{in}^n \times C_b^n L^b - C_b^n \omega_{ib}^b \times L^b \right) + v_v \quad (3.5)$$

The attitude error measurement uses the DCM matching method. Since DCMs are  $3 \times 3$  matrices, the measurement can be defined in a matrix equation as



$$Z_{DCM} = \hat{C}_S^n \hat{C}_M^S \hat{C}_n^M - C_S^n C_M^S C_n^M \quad (3.6)$$

and using the following property of DCM,

$$C_S^n C_M^S C_n^M = I \quad (3.7)$$

the measurement equation yields

$$Z_{DCM} = [I - \Psi] C_S^n [I - \Phi] C_M^S [I - v_\theta \times] C_n^M - I \quad (3.8)$$

where,  $v_\theta \times$  is the attitude error of the MINS, which can be expressed as the Gaussian noise, because it assumed to a very small error. Neglecting the error product terms, the DCM error will be:

$$Z_{DCM} = C_S^n C_M^S C_n^M - \Psi C_S^n C_M^S C_n^M - C_S^n \Phi C_M^S C_n^M - C_S^n C_M^S [v_\theta \times] C_n^M - I \quad (3.9)$$

Then the matrix measurement equation is simplified into

$$Z_{DCM} = -\Psi - C_S^n \Phi C_S^{nT} + [v_\phi \times] \quad (3.9)$$

Thus, the attitude error measurement can be expressed in vector form as:

$$z_{DCM} = -\psi - C_s^n \phi + v_\theta \quad (3.10)$$

Then the measurement equation and measurement matrix for extended Kalman filter is

$$z = \begin{bmatrix} V^{n,M} - \hat{V}^{n,M} \\ -\psi - C_s^n \phi \end{bmatrix} + \begin{bmatrix} v_v \\ v_\theta \end{bmatrix} \quad (3.11)$$

$$H = \begin{bmatrix} I & 0 & 0 & 0 & 0 \\ 0 & -I & -C_b^n & 0 & 0 \end{bmatrix}$$

The mis-alignment must be estimated to consider flexure effect. By observability analysis, it is known that the acceleration of the launcher must be performed to make the sensor bias states observable.

### 3.2 Performance Analysis of Conventional Alignment

The most important factor of performance of transfer alignment is yaw error. Roll and pitch error converge rapidly, however, yaw error converges very slowly under launcher with lack of observability. Observability is

affected by maneuver of launcher. This characteristics can be proved by observability analysis of EKF (extended Kalman filter). The observability of time varying nonlinear system is defined to total observability [45, 46].

The observability matrix is defined as following equation.

$$O = \begin{bmatrix} H \\ HF \\ HF^2 \\ \vdots \\ HF^{N-1} \end{bmatrix} \quad (3.12)$$

When the observability matrix has full rank, all states can be properly estimated. On the steady state vehicle, the product of measurement matrix and system matrix is derived as:

$$H = \begin{bmatrix} I & 0 & 0 & 0 & 0 \\ 0 & -I & -C_b^n & 0 & 0 \end{bmatrix} \quad (3.13)$$

$$HF = \begin{bmatrix} F_{11} & F_{12} & 0 & F_{14} & 0 \\ -F_{21} & -F_{22} & 0 & 0 & -F_{25} \end{bmatrix} \quad (3.14)$$

$$HF^2 = \begin{bmatrix} F_{11}^2 + F_{12}F_{21} & F_{11}F_{12} + F_{12}F_{22} & 0 & F_{11}F_{14} & F_{12}F_{25} \\ -F_{21}F_{11} - F_{22}F_{21} & -F_{21}F_{12} - F_{22}^2 & 0 & -F_{21}F_{14} & -F_{22}F_{25} \end{bmatrix} \quad (3.15)$$

$$HF^3 = \begin{bmatrix} F_{11}^3 + F_{12}F_{21}F_{11} + F_{11}F_{12}F_{21} + F_{12}F_{22}F_{21} & F_{11}^2F_{12} + F_{12}F_{21}F_{12} + F_{11}F_{12}F_{22} + F_{12}F_{22}^2 & 0 & F_{11}^2F_{14} + F_{12}F_{21}F_{14} & F_{11}F_{12}F_{25} + F_{12}F_{22}F_{25} \\ -F_{21}F_{11}^2 - F_{22}F_{21}F_{11} - F_{21}F_{12}F_{21} - F_{22}^2F_{21} & -F_{21}F_{11}F_{12} - F_{22}F_{21}F_{12} - F_{21}F_{12}F_{22} - F_{22}^3 & 0 & -F_{21}F_{11}F_{14} - F_{22}F_{21}F_{14} & -F_{21}F_{12}F_{25} - F_{22}^2F_{25} \end{bmatrix} \quad (3.16)$$

Then the observability matrix can be expressed as:

$$O = \begin{bmatrix} I & 0 & 0 & 0 & 0 \\ 0 & -I & -C_b^n & 0 & 0 \\ F_{11} & F_{12} & 0 & F_{14} & 0 \\ -F_{21} & -F_{22} & 0 & 0 & -F_{25} \\ F_{11}^2 + F_{12}F_{21} & F_{11}F_{12} + F_{12}F_{22} & 0 & F_{11}F_{14} & F_{12}F_{25} \\ -F_{21}F_{11} - F_{22}F_{21} & -F_{21}F_{12} - F_{22}^2 & 0 & -F_{21}F_{14} & -F_{22}F_{25} \\ \vdots & \vdots & \vdots & \vdots & \vdots \end{bmatrix} \quad (3.17)$$

By using Gauss elimination, the independent terms of the observability matrix can be expressed as:

$$O' = \begin{bmatrix} I & 0 & 0 & 0 & 0 \\ 0 & -I & -C_b^n & 0 & 0 \\ \hline 0 & F_{12} & 0 & F_{14} & 0 \\ 0 & -F_{22} & 0 & 0 & -F_{25} \\ \hline 0 & 0 & 0 & 0 & 0 \\ 0 & 0 & 0 & 0 & 0 \end{bmatrix} \quad (3.18)$$

And the highest rank of the observability matrix is 12.

$$\max(\text{rank}(O)) = 12 < 15 \quad (3.19)$$

Thus, only a maximum 12 states are can be estimated in an application that involves a steady state vehicle. To prove these results, simulations of the transfer alignment of the steady state was conducted. The total simulation time was 180 seconds, and the performance of the inertial measurement units used for simulations are summarized as follows.

- Sampling rate : 100Hz
- Accelerometer bias of MINS :  $10 \mu g$
- Accelerometer bias of SINS :  $100 \mu g$
- Gyro bias of MINS :  $0.01 \text{ deg/hr}$
- Gyro bias of SINS :  $0.1 \text{ deg/hr}$

The true misalignment angle is set to one degree for all axes, and the attitude error result is expressed in the figures below..

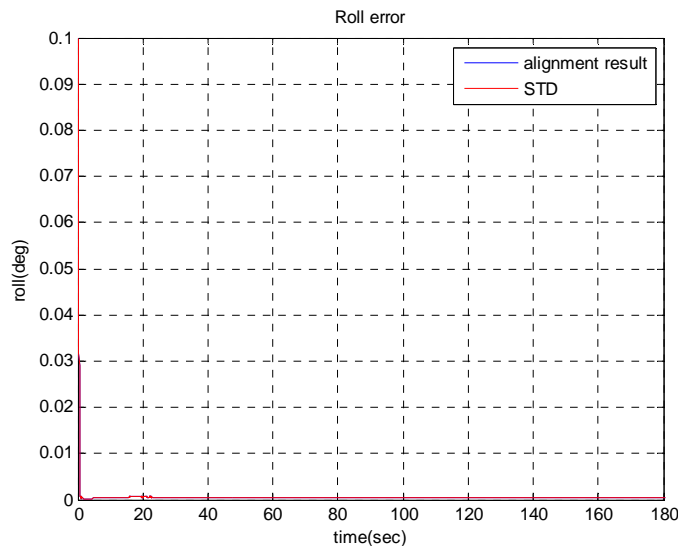


Figure 7. Roll error of transfer alignment on stationary vehicle

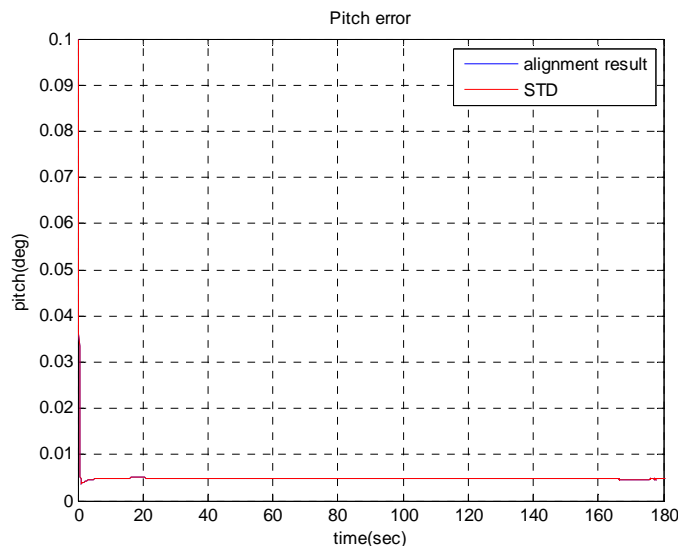


Figure 8. Pitch error of transfer alignment on stationary vehicle

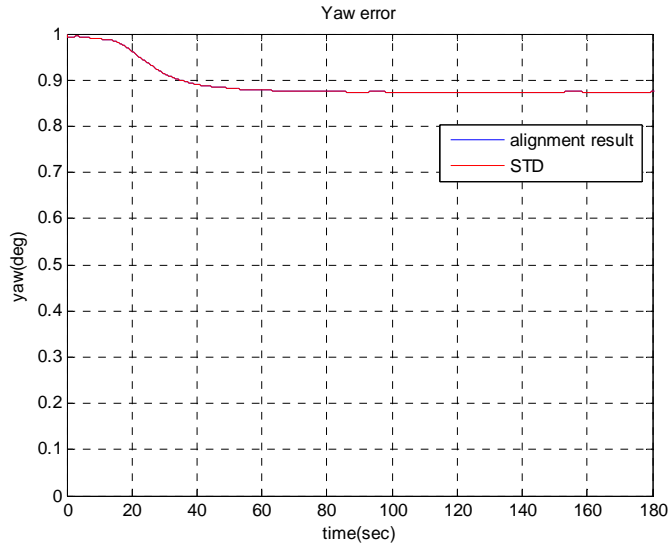


Figure 9. Yaw error of transfer alignment on stationary vehicle

As predicted, roll and pitch error are properly estimated. Yaw angle error converged in the first 60 seconds. However, it settled on about 0.87 degrees, and, that is, the steady state yaw estimation accuracy is too low to be used for inertial navigation. Thus, most launchers requires to perform maneuvers, so that the motion of the vehicle allows for a smaller error of estimation.

For a ground vehicle, the following figure shows the yaw result of the transfer alignment under a simple attitude maneuver. In this case, the yaw of the launcher rotated from 30 to 40 seconds with an angular rate of 10 deg/sec.

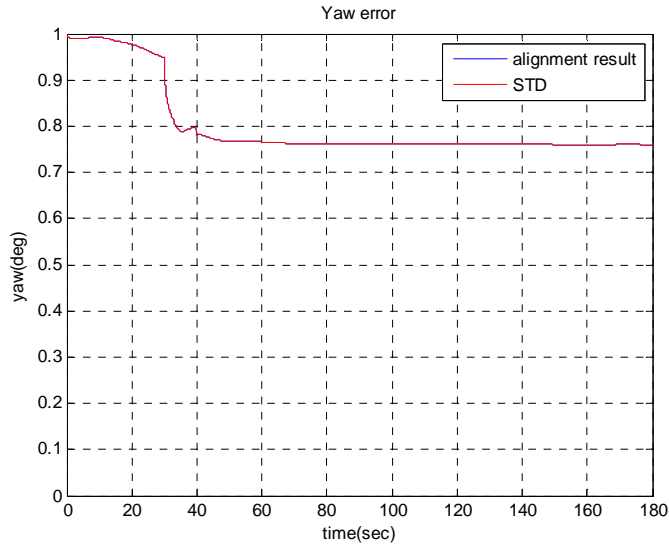


Figure 10. Yaw error of transfer alignment under attitude maneuver

Though the performance increased relative to the steady state result, the yaw angle still cannot be properly estimated. The velocity change of the MINS is generated by the lever arm effect only. So, the observability of the filter cannot be sufficiently improved.

When the attitude maneuver is conducted for a long time, the yaw estimation performance can be improved. In the following simulation results, the yaw of the launcher rotated from 30 seconds to 5 minutes with a rate of 10 deg/sec.



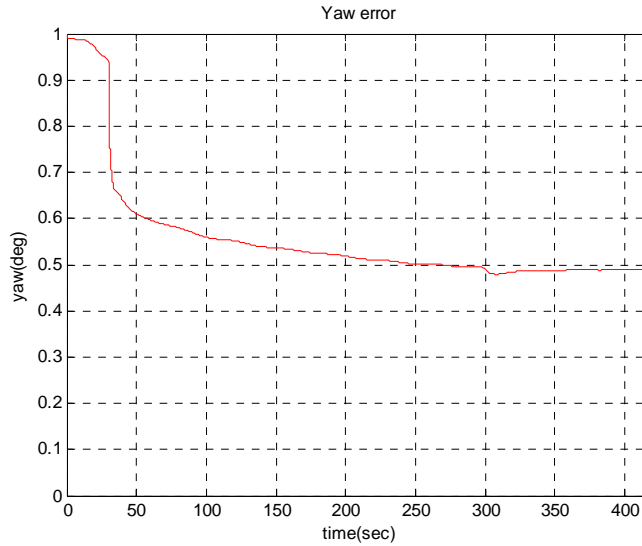


Figure 11. Yaw error of transfer alignment under long attitude maneuver

Figure 11 shows the yaw estimation result for 7 minutes. When the maneuver started at 30 second, the yaw error converged rapidly in the initial stage, and the error convergence rate decreased gradually. After a 5-minute maneuver, the total error was 0.5 degrees. Although, this is a better result than that of the short maneuver, it still has insufficient precision for many applications.

On the other hand, the acceleration motion of the vehicle can have a dominant effect in improving observability. The following figure shows the result of the transfer alignment on an accelerating vehicle.

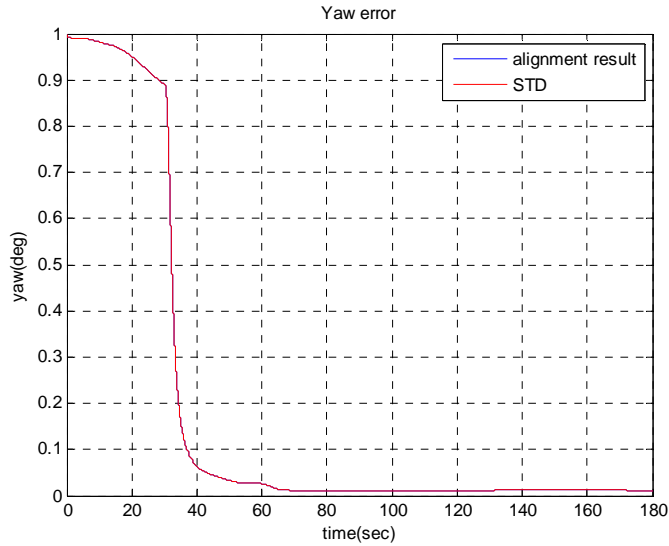


Figure 12. Yaw error of transfer alignment under acceleration maneuver

The MINS accelerated for 1m/s from 30 to 60 seconds. The attitude error rapidly converged after 30 seconds, and the final attitude error was maintained at under 0.05 degrees. In effect, acceleration motion is essential for proper performance of the transfer alignment. However, it is impossible for most ground based launchers to conduct acceleration maneuvers during an emergency situation. Thus, a novel method for transfer alignment must be developed for use in ground launchers.

### 3.3 New Amplitude Measurement using Vibration of the Vehicle

### 3.3.1 Simplified Attitude Error Equation for Amplitude Measurement

The purpose of the transfer alignment is to figure out the relative attitude between a SINS and a MINS. The typical algorithm matches the attitude and velocity of a SINS and a MINS. The proposed alignment method uses the vibration of the vehicle to estimate the misalignment angles by using the amplitude of the raw inertial sensor signals. The SINS and MINS sensor signals can be represented by Eqs. (92) and (93) below, respectively, as

$$\bar{s}^S = s^S + \delta s^S \quad (3.20)$$

$$\bar{s}^M = s^M + \delta s^M \quad (3.21)$$

where  $\bar{s}^S$  is the measurement of the SINS (which can be the accelerometer or gyro output),  $s^S$  is the true signal containing the sinusoidal components generated by the vibration of the vehicle, and  $\delta s^S$  is the sensor error term of the SINS composed of the bias, white noise, and low frequency term drifting with the Markov process. The superscripts S and M refer to the signals of the SINS and MINS respectively, so that, for example,  $s^M$  is the true signal of the MINS.

Let us assume that the SINS and the MINS are assembled within a single

rigid body. The relative attitude between the SINS and the MINS is then a fixed value which is referred to as the misalignment angle. Since the sinusoidal components of the true signals come from the vibration of the vehicle,  $s^S$  is equal to attitude transformation of  $s^M$ . The misalignment angle between the SINS and MINS is represented as the direction cosine matrix  $C_M^S$ , which has a fixed value.  $s^S$  is then expressed by  $s^M$  and  $C_M^S$  as

$$s^S = C_M^S s^M \quad (3.22)$$

The estimate of  $C_M^S$  is represented as  $\hat{C}_M^S$ , which contains the misalignment angle  $\Phi$  and is derived as

$$\hat{C}_M^S = [I - \Phi] C_M^S \quad (3.23)$$

where the mis-alignment angle matrix is defined as the skew-symmetric matrix.

$$\Phi = \begin{bmatrix} 0 & -\gamma & \beta \\ \gamma & 0 & -\alpha \\ -\beta & \alpha & 0 \end{bmatrix} \quad (3.24)$$

$C_M^S$  can be derived from Eq. (3.23).

$$C_M^S = \hat{C}_M^S + \Phi C_M^S \quad (3.25)$$

Eq. (3.22) can be transformed to the error equation.

$$\bar{s}^S = \left( \hat{C}_M^S + \Phi C_M^S \right) \left( \bar{s}^M - \delta s^M \right) + \delta s^S \quad (3.26)$$

Ignoring the higher terms in Eq. (3.26), the attitude error equation will be:

$$\bar{s}^S \approx \hat{C}_M^S \bar{s}^M - \hat{C}_M^S \delta s^M + \Phi C_M^S \bar{s}^M + \delta s^S \quad (3.27)$$

### 3.3.2 EKF based Transfer Alignment using Amplitude

Transfer alignment using the vibration of the vehicle is derived from the amplitude of the SINS and MINS, which can be obtained via a discrete Fourier transform (DFT)[47]. The DFT of each of the signals at  $\omega_i$  are defined as:

$$\mathbb{F}[\bar{s}^S]_{\omega=\omega_1} = \bar{S}^S(\omega_1) \quad (3.28)$$

$$\mathbb{F}[\hat{C}_M^S \bar{s}^M]_{\omega=\omega_1} = \hat{S}^S(\omega_1) \quad (3.29)$$

$$\mathbb{F}[\delta s^S]_{\omega=\omega_1} = V^S(\omega_1) \quad (3.30)$$

where,  $\omega_1$  is  $2\pi f_1$  and  $f_1$  is the frequency of the vibration of the vehicle.

After performing a DFT for both sides of Eq. (3.27), it can be transformed to

$$\bar{S}^S(\omega_1) = \mathbb{F}[\hat{C}_M^S \bar{s}^M] - \mathbb{F}[\hat{C}_M^S \delta s^M] + \mathbb{F}[\Phi C_M^S \bar{s}^M] + \mathbb{F}[\delta s^S] \quad (3.31)$$

On the right hand of Eq. (13), only  $\bar{s}^M$  has a significantly large value at frequency  $f_1$ . Since  $\hat{C}_M^S$  is composed of the attitude error and fixed misalignment angle,  $\hat{C}_M^S$  can be treated as a constant.  $\delta s^M$  also has a very small value under the assumption that the MINS is much more accurate than the SINS.

$$\mathbb{F}[\delta s^M]_{\omega_1} \approx 0 \quad (3.32)$$

Consequently, Eq. (3.32) can be simplified as

$$\bar{S}^s(\omega_1) = \hat{S}^s(\omega_1) + \Phi C_M^s \bar{S}^M(\omega_1) + V^s(\omega_1) \quad (3.33)$$

Therefore,

$$\bar{S}^s(\omega_1) = [I + \Phi] \hat{S}^s(\omega_1) + V^s(\omega_1) \quad (3.34)$$

The amplitude of Eq. (106) can be calculated as

$$|\bar{S}^s(\omega_1)|^2 = |[I + \Phi] \hat{S}^s(\omega_1) + V^s(\omega_1)|^2 \quad (3.35)$$

Each signal of  $\hat{S}^s(\omega_1)$  for each axis is expressed as having real and imaginary parts.

$$\begin{aligned} \hat{S}_x^s(\omega_1) &= a_x + b_x i, \\ \hat{S}_y^s(\omega_1) &= a_y + b_y i, \\ \hat{S}_z^s(\omega_1) &= a_z + b_z i. \end{aligned} \quad (3.36)$$

Then the x-axis signal can be derived as:

$$\left| \bar{S}_x^s(\omega_1) \right|^2 = \left| a_x + b_x i - \gamma(a_y + b_y i) + \beta(a_z + b_z i) + V_x^s(\omega_1) \right|^2 \quad (3.37)$$

Without second-order error terms, Eq. (3.37) is modified into

$$\left| \bar{S}_x^s(\omega_1) \right|^2 = (a_x - \gamma a_y + \beta a_z)^2 + (b_x - \gamma b_y + \beta b_z)^2 + v_x(\omega_1) \quad (3.38)$$

where,  $V_x$  is the error term generated by the white noise of the SINS. It is defined as

$$v_x = 2a_x^2 \text{real}(v_x^s(\omega_1))^2 + 2b_x^2 \text{imag}(v_x^s(\omega_1))^2 \quad (3.39)$$

The phase of the white noise is not meaningful. When the real and imaginary parts of  $v_x^s(\omega_1)$  are assumed to have similar values,  $v_x$  can be defined as

$$v_x \approx 4 \left| \hat{S}_x^s(\omega_1) \right|^2 \left| v_x^s(\omega_1) \right|^2 \quad (3.40)$$

Similar to Eq. (3.38), the amplitudes of the other axes can be derived as



$$\left| \bar{S}_y^s(\omega_1) \right|^2 = (\gamma a_x + a_y - \alpha a_z)^2 + (\gamma b_x + b_y - \alpha b_z)^2 + v_y \quad (3.41)$$

$$\left| \bar{S}_z^s(\omega_1) \right|^2 = (-\beta a_x + \alpha a_y + a_z)^2 + (-\beta b_x + \alpha b_y + b_z)^2 + v_z \quad (3.42)$$

The proposed algorithm uses these squared amplitudes as vector measurements for the Kalman filter. With respect to the estimation of the attitude using a vector measurement, the attitude cannot be estimated with only one measurement because of the lack of observability. Thus, the proposed method requires two distinguishable vibration sources operating at different frequencies. Many ground-based launchers have two or more potential sources of vibration such as engines and generators. The frequency of vibrations should be defined via analysis of vehicle dynamics.

To compute the amplitude using DFT, signal measurements must be continuously collected for specific time intervals. The time interval should be adjusted to have sufficient frequency resolution. If the interval is too short, the amplitude peaks of the signal are divided into several frequency bands, resulting in significant errors in attitude estimation. If the time interval is too long, though, the measurement for each time interval might be more accurate, but the performance of the filter deteriorates due to the lower number of

measurements taken.

There are two important remarks to make respect to the new alignment method.

**Remark 1 :** Using this new alignment method, the performance of the SINS accelerometer has less effect on the attitude estimate than it does when using typical algorithms. The sensor error  $\delta s^s$  is composed of the bias and low frequency drift and white noise on all frequencies. Of those errors, only white noise can exist in the high frequency band. Since Eq. (3.38) only contains error terms related to  $\omega_1$ , bias and low frequency terms cannot affect the measurement, and only high frequency noise can degrade the performance of the transfer alignment. On the other hand, using the typical transfer alignment algorithm, the final attitude estimation error after convergence is determined by the accelerometer bias.

**Remark 2 :** The new amplitude measurement does not use the error measurement. Most of the Kalman filters for transfer alignment usually use the error measurement by subtracting the velocity of the MINS from velocity of the SINS. If the error measurement of  $\bar{S}^s(\omega_1) - \hat{S}^s(\omega_1)$  is used in the proposed algorithm, the delay and phase differences between the SINS and the MINS can create a critical problem. However, the proposed method uses a direct measurement of the squared amplitude of the MINS and the SINS. This

causes the Kalman filter to be robust against delay between the SINS and MINS signals.

### 3.3.3 Transfer Alignment Algorithm using Two Vibrations

The proposed filter structure is illustrated in the figure below.

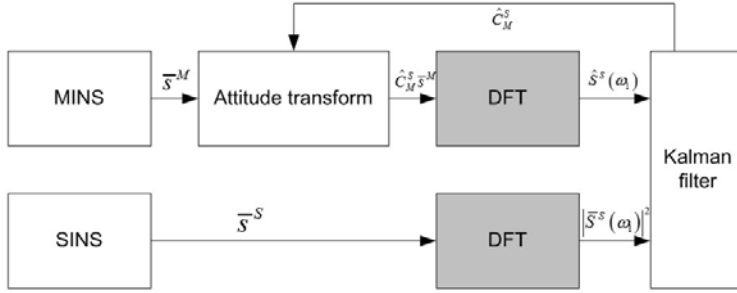


Figure 13. Proposed Alignment Structure

With the new amplitude measurements, the misalignment error can be estimated using EKF. The states are defined to be mis-alignment angles by

$$x = [\alpha \quad \beta \quad \gamma]^T \quad (3.43)$$

As the misalignment angle is fixed, the process model can be expressed

as

$$\dot{x} = 0 \quad (3.44)$$

The proposed amplitude measurement is used as a measurement. As stated above, two sources of vibration with different frequencies are required in order to estimate the misalignment angle.

$$z = \left[ |S_x^s(\omega_1)|^2 \quad |S_y^s(\omega_1)|^2 \quad |S_z^s(\omega_1)|^2 \quad |S_x^s(\omega_2)|^2 \quad |S_y^s(\omega_2)|^2 \quad |S_z^s(\omega_2)|^2 \right]^T \quad (3.45)$$

To implement to EKF, the linearized measurement matrix is given as

$$H = \frac{\partial z}{\partial x} = \begin{bmatrix} 0 & 2a_z(\omega_1) + 2b_z(\omega_1) & -2a_y(\omega_1) - 2b_y(\omega_1) \\ -2a_z(\omega_1) - 2b_z(\omega_1) & 0 & 2a_x(\omega_1) + 2b_x(\omega_1) \\ 2a_y(\omega_1) + 2b_y(\omega_1) & -2a_x(\omega_1) - 2b_x(\omega_1) & 0 \\ 0 & 2a_z(\omega_2) + 2b_z(\omega_2) & -2a_y(\omega_2) - 2b_y(\omega_2) \\ -2a_z(\omega_2) - 2b_z(\omega_2) & 0 & 2a_x(\omega_2) + 2b_x(\omega_2) \\ 2a_y(\omega_2) + 2b_y(\omega_2) & -2a_x(\omega_2) - 2b_x(\omega_2) & 0 \end{bmatrix} \quad (3.46)$$

The proposed algorithm is summarized as follows.

- 1) Using the product of the MINS accelerometer signals and the estimated direction cosine matrix  $\hat{C}_M^s$ ,  $\hat{C}_M^s \bar{s}^M$  is computed in the time domain.

- 2)  $\hat{C}_M^S \bar{s}^M$  is collected for a fixed interval and is transformed to the frequency domain using DFT.
- 3) The SINS accelerometer signals are transformed to the frequency domain.
- 4) At frequency  $f_1$  and  $f_2$ , the squared amplitudes are computed.
- 5) The attitude is estimated by means of EKF using the computed amplitudes.

### 3.3.4 Simulational Result

To verify the proposed algorithm, a transfer alignment simulation was conducted. The total simulation time was 100 seconds, and the performance of the inertial measurement units used for the simulation is summarized as follows.

- Sampling rate : 100Hz
- Accelerometer bias of MINS :  $100 \mu g$
- Accelerometer bias of SINS :  $1000 \mu g$
- Gyro bias of MINS :  $0 \text{ deg/hr}$
- Gyro bias of SINS :  $1 \text{ deg/hr}$

The true misalignment angle is set to one degree for all axes. The

vibration source chosen for the simulation is that of a car as expressed in Fig.

13.

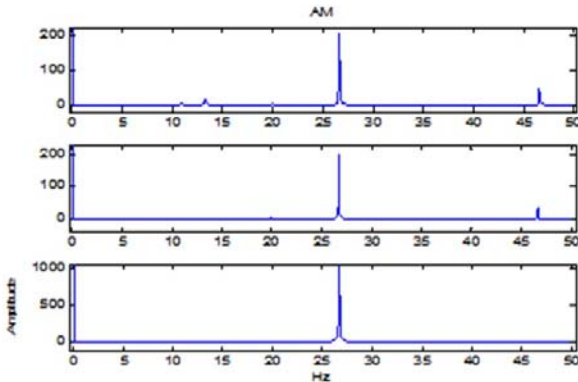


Figure 14. Amplitude of vibration of a car

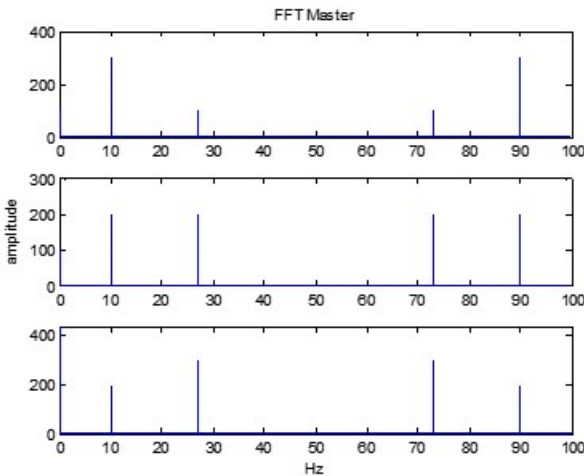


Figure 15. Simulated signal

The vibration of the vehicle has a significantly large peak at the

frequency of the engine vibration. The amplitude of the simulated accelerometer signal is seen in Fig. 14, and the acceleration of each axis is as follows:

$$s^M = \begin{bmatrix} 0.03 \sin(2\pi f_1 t) - 0.05 \sin(2\pi f_1 t + \pi / 4) \\ 0.02 \sin(2\pi f_1 t) - 0.06 \sin(2\pi f_1 t + \pi / 4) \\ 0.01 \sin(2\pi f_1 t) - 0.07 \sin(2\pi f_1 t + \pi / 4) \end{bmatrix} \quad (3.47)$$

This vibration produced by the car engine is too small to be useful for a typical transfer alignment algorithm. Using a typical attitude and velocity matching method, the yaw angle cannot be estimated due to a lack of observability. The result of the conventional transfer alignment can be viewed in the figure below.

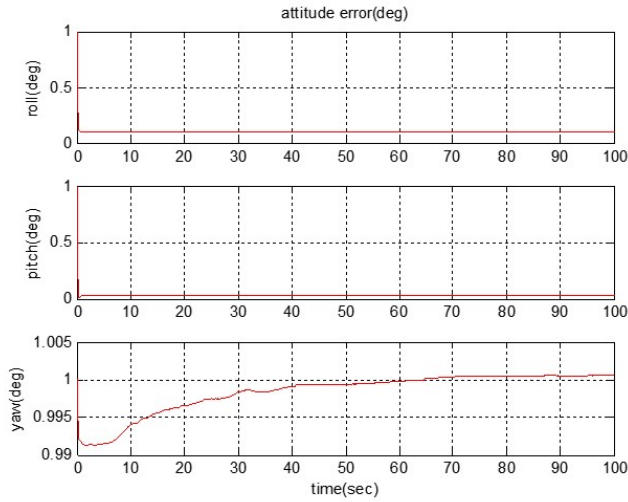


Figure 16. Transfer alignment result of conventional algorithm

In the simulation results shown in Fig. 16, the roll and pitch errors converge to specific values. However, the yaw error does not converge with time. In this case, the engine vibration generates a small but insignificant amount of movement for alignment, so the vehicle can be said to be in a fundamentally stationary state. Several previous studies have noted that a transfer alignment conducted on a launcher-projectile system mounted on a vehicle in a steady state results in low performance in yaw angle estimation.

The simulation results of the proposed algorithm are shown in Fig. 17.

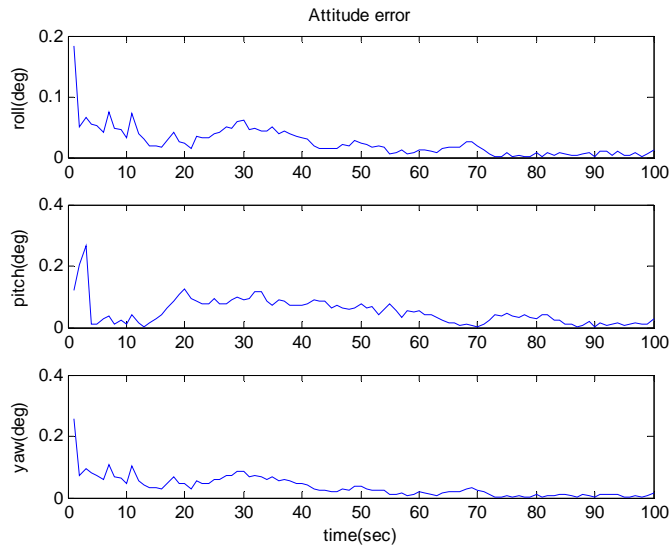


Figure 17. Simulation results of the proposed algorithm



100 samples were gathered for DFT at one-second intervals and were transformed to the frequency domain. In this case, the 3 axes of attitude properly converged with time, and the alignment error converged to zero. Unlike previous studies, the yaw angle is properly estimated with the proposed algorithm. The convergence time of the roll and pitch angles when using the proposed method is longer than that when using a typical method due to a decrease in the number of measurements used. One amplitude measurement is computed for each time interval, an only 100 samples of data are available for 100 seconds. However, the accuracy of the measurements is greater owing to the reason noted in the above remark 2.

This work shows the possibility of having a new means of taking measurements for alignment. However, there are four problems in using this algorithm. At first, the proposed algorithm requires two different sources of vibration. Though some vehicles have two vibration sources, like an engine and a power generator, most of vehicles have only one vibration source. The second problem is that the proposed method assumes the connector between launcher and the projectile is a rigid body. To apply in real systems, damping of the vibration must be considered. And the third problem is that roll and pitch estimation performance of the proposed method are degraded relative to the conventional method. The final problem is that the proposed algorithm can

estimate only misalignment angles. To improve performance of the estimation, other factors such as sensor bias must be taken into account.

So, in order to solve these problems, new measurements are integrated into a conventional velocity and attitude matching transfer alignment system.

### **3.3 Transfer Alignment Method using Frequency Domain Approach**

The proposed algorithm uses the filter structure of a conventional velocity and attitude matching transfer alignment algorithm, and the proposed amplitude measurement is augmented with the measurement model. Then, problems of two-vibration alignment can be resolved. At first, only one vibration is required. Since roll and pitch angle are able to be properly estimated by the conventional filter structure, only yaw angle is estimated by the vibration measurement. As stated in the previous section, two different vectors are required to estimate the attitude with vector measurement. In this case, the gravity vector can be an additional vector measurement. The second advantage is that roll and pitch angle estimation performance will increase. Roll and pitch angle estimation performance of the two-vibration alignment is less effective than that of the conventional method because the vibration measurement uses only the high frequency component of the accelerometer.

However, if the amplitude measurement is augmented with the conventional algorithm, the roll and pitch angle can be estimated with a low frequency signal. The third advantage is that sensor bias can be estimated because the same filter structure as that of conventional algorithm can be used.

The entire algorithm is illustrated in figure 17.

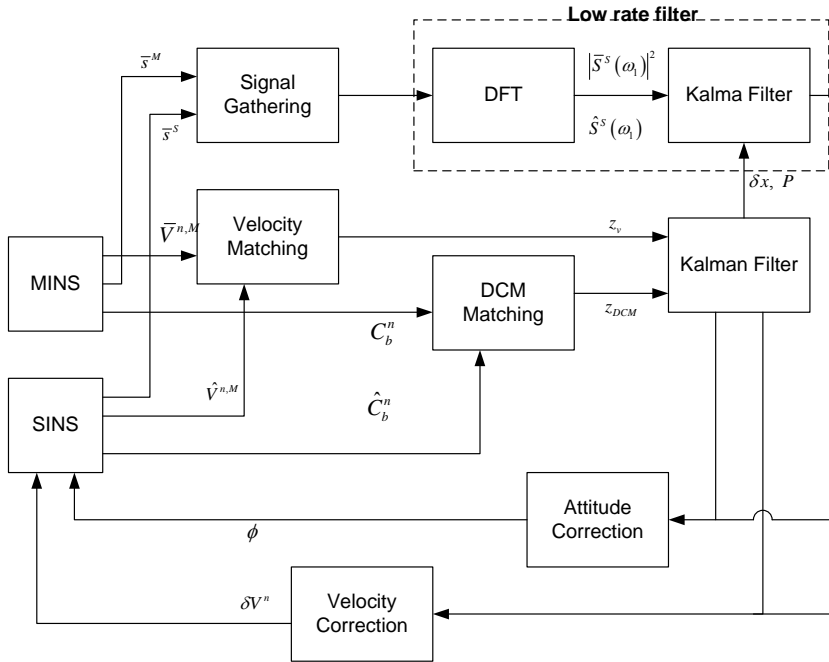


Figure 18. Filter structure of amplitude measurement augmented transfer alignment

Sampling rate of conventional velocity and attitude measurement are high (set to 100Hz in the simulation). However, the sampling rate of the

amplitude measurement is low (set to 1Hz in the simulation) by signal gathering for DFT. Thus the measurement update for a conventional measurement and the measurement update for amplitude are conducted with different rates.

The process model of the proposed algorithm is the same as a process model of the conventional algorithm described in (3.2). The state variables are velocity error  $\delta V^n$ , attitude error  $\psi$ , mis-alignment error  $\phi$ , accelerometer biases  $\nabla$ , and gyro biases  $\varepsilon$ .

$$\delta x = \begin{bmatrix} \delta V^{nT} & \psi^T & \phi^T & \nabla^T & \varepsilon^T \end{bmatrix}^T \quad (3.48)$$

The process model is

$$\delta \dot{x} = F \delta x + w \quad (3.49)$$

The system matrix  $F$  is the same as the matrix expressed in section 3.1. State variables are updated for high frequency according to the sampling rate of MINS and SINS.

The measurement equation of the high rate filter is the same as that in section 3.1 as well.

$$z_1 = \begin{bmatrix} V^{n,M} - \hat{V}^{n,M} \\ -\psi - C_S^n \phi \end{bmatrix} + \begin{bmatrix} v_v \\ v_\theta \end{bmatrix} \quad (3.50)$$

And the low rate measurement equation uses the amplitude equation (3.45).

$$z_2 = \begin{bmatrix} |S_x^s(\omega_1)|^2 & |S_y^s(\omega_1)|^2 & |S_z^s(\omega_1)|^2 \end{bmatrix}^T \quad (3.51)$$

After the low rate filter update, position, velocity, attitude should be corrected in order to compute the local gravity vector, transport rate, and local Earth rate in the similar manner to the conventional transfer alignment.

As another important property of the proposed transfer alignment, the damping effect need to be considered. To consider damping between the launcher and the projectile, the following assumption is required.

**Assumption** : The transmissibility of the vibration is fixed for each axis. If the projectiles are installed on a fixed point on the launcher, transmissibility does not significantly change after each trial because dampers and vibration isolators remain same. Thus, the engineer can measure transmissibility in advance, and these characteristics can be applied to the transfer alignment.

Transmissibility  $T$  is defined as:

$$T = \left| \frac{A_o}{A_i} \right| \quad (3.52)$$

where,  $A_o$  is amplitude of the vibrational response, and  $A_i$  is amplitude of the vibrational input. To apply to transfer alignment, transmissibility of each axis is defined by experiments beforehand. Using the transmissibility of each axis as  $T_x, T_y, T_z$ , the measurement equation (3.51) yields :

$$\left| \bar{S}_x^S(\omega_1) \right|^2 = \left( T_x a_x - T_y \gamma a_y + T_z \beta a_z \right)^2 + \left( T_x b_x - T_y \gamma b_y + T_z \beta b_z \right)^2 + v_x \quad (3.53)$$

$$\left| \bar{S}_y^S(\omega_1) \right|^2 = \left( T_x \gamma a_x + T_y a_y - T_z \alpha a_z \right)^2 + \left( T_x \gamma b_x + T_y b_y - T_z \alpha b_z \right)^2 + v_y \quad (3.54)$$

$$\left| \bar{S}_z^S(\omega_1) \right|^2 = \left( -T_x \beta a_x + T_y \alpha a_y + T_z a_z \right)^2 + \left( -T_x \beta b_x + T_y \alpha b_y + T_z b_z \right)^2 + v_z \quad (3.55)$$

If the transmissibility does not change with time, then the transfer alignment with amplitude measurement can be applied to real systems.

### 3.4 Simulation Results

For verification of the proposed algorithm, transfer alignment

simulations were conducted. The total simulation time was 180 seconds, and the performance of the inertial measurement units used for the simulation is summarized as follows.

- Sampling rate : 100Hz
- Accelerometer bias of MINS :  $10 \mu g$
- Accelerometer bias of SINS :  $100 \mu g$
- Gyro bias of MINS :  $0.01 \text{ deg/hr}$
- Gyro bias of SINS :  $0.1 \text{ deg/hr}$
- Number of samples for block processing of DFT : 100
- Mis-alignment angle : 1deg for roll, pitch, and yaw
- Transmissibility :  $T_x = 0.5$ ,  $T_y = 0.4$ ,  $T_z = 0.3$

The vibration of vehicle is represented as:

$$V^{b,M} = \begin{bmatrix} 0.3 \cos(27 \times 2\pi t) & 0.2 \cos(27 \times 2\pi t) & 0.1 \cos(27 \times 2\pi t) \end{bmatrix} \quad (3.54)$$

At first, to verify the performance of the conventional transfer alignment of this system, the conventional transfer alignment simulation is conducted without amplitude measurement.

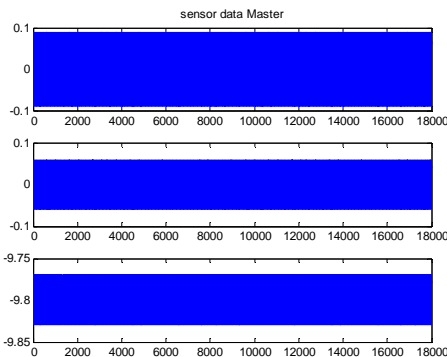


Figure 19. Accelerometer measurement on the vibrating vehicle

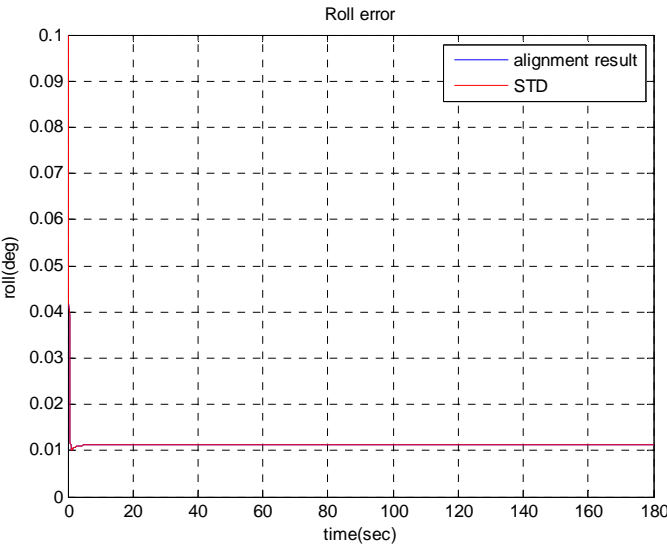


Figure 20. Roll error result of the conventional transfer alignment for the  
vibrating vehicle



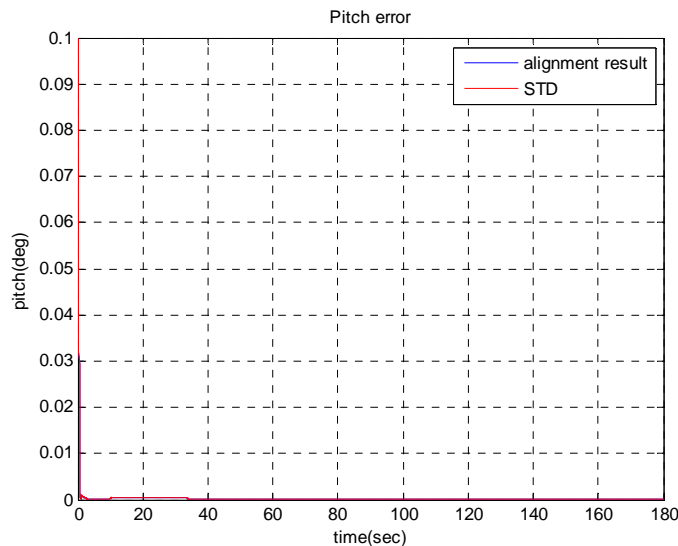


Figure 21. Pitch error result of the conventional transfer alignment for the vibrating vehicle

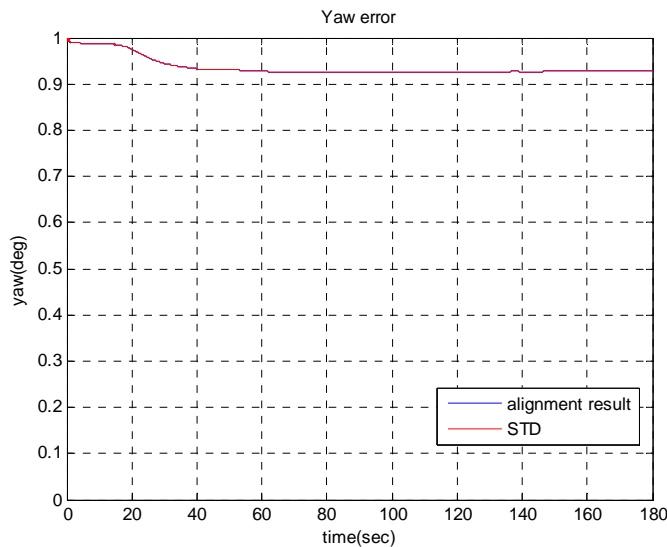


Figure 22. Yaw error result of the conventional transfer alignment for the vibrating vehicle

As shown in section 3.2, the acceleration of vehicle increases the observability of the transfer alignment. As shown in Figure 19, acceleration exists by result of the vibration. However, even the vehicle is accelerating, yaw angle cannot be properly estimated because the acceleration is too small. In Figure 20 and 21, the roll and pitch angle error converges to 0, but the yaw angle error shows error of more than 0.9 degrees in Figure 22.

The results of the amplitude measurement augmented algorithm of the same vehicle are shown in the following figures.

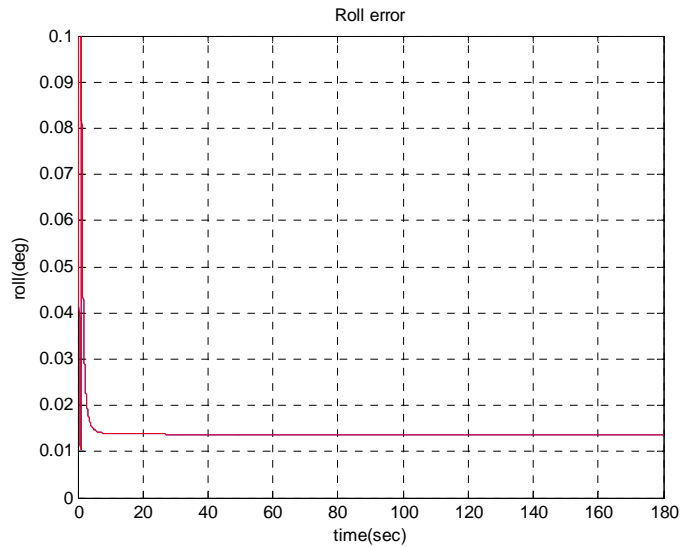


Figure 23. Roll error of the proposed algorithm

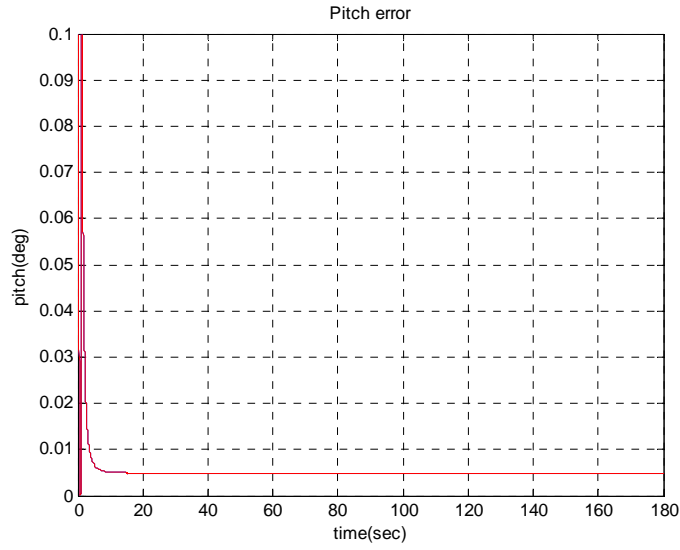


Figure 24. Pitch error of the proposed algorithm

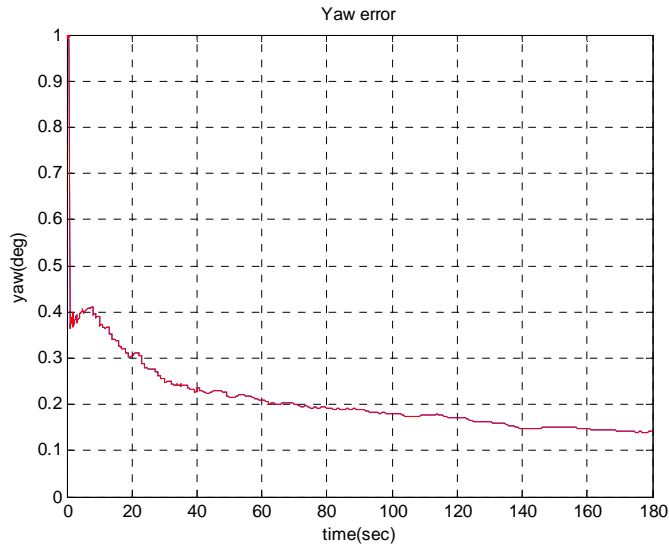


Figure 25. Yaw error of the proposed algorithm

As shown in Figure 25, the yaw angle estimation performance

significantly increased. With the conventional algorithm, yaw error cannot be converged, but the yaw error of the proposed algorithm converges with time. The yaw error converges in a step-like manner, and this characteristics is due to the low update rate of measurement. Since amplitude measurements are measured by 1 sec, the yaw error is compensated at every second.

However, there are some drawbacks to using this algorithm. At first, the roll and pitch error slightly increase, due to the augmented amplitude measurement. The amplitude measurement can be largely affected by noise, because it uses a high frequency signal. To eliminate the effect on the roll and pitch angles, a two-stage filter needs to be considered for development in future work.

Another problem of the proposed method is caused by the measurement configuration. Let's consider vibration described by the following.

- Transmissibility :  $T_x = T_y = T_z = 0.2 = T$

- Amplitude of Vibration :  $|V^{b,M}| = [0.1 \ 0.1 \ 0.1]$

The yaw error result is expresses in Figure 26.

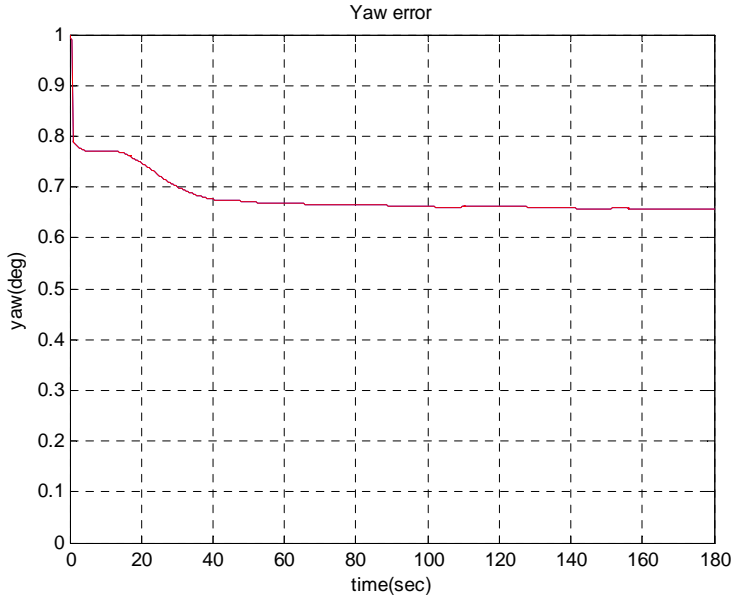


Figure 26. Amplitude dependency problem

In this case, the amplitude measurement of each axis is the same. Then the measurement matrix of the amplitude measurement filter can be derived as:

$$H = \frac{\partial z}{\partial x} = \begin{bmatrix} 0 & 2T_z a_z(\omega_1) + 2T_z b_z(\omega_1) & -2T_y a_y(\omega_1) - 2T_y b_y(\omega_1) \\ -2T_z a_z(\omega_1) - 2T_z b_z(\omega_1) & 0 & 2T_x a_x(\omega_1) + 2T_x b_x(\omega_1) \\ 2T_y a_y(\omega_1) + 2T_y b_y(\omega_1) & -2T_x a_x(\omega_1) - 2T_x b_x(\omega_1) & 0 \end{bmatrix} \quad (3.55)$$

Since the amplitude of each axis is the same, the measurement of the equation can be simplified to:

$$H = \frac{\partial z}{\partial x} = T(2a + 2b) \begin{bmatrix} 0 & 1 & -1 \\ -1 & 0 & 1 \\ 1 & -1 & 0 \end{bmatrix} \quad (3.56)$$

This measurement matrix has a dependency in the rows and observability drastically decrease. Thus, the yaw estimation performance decrease.

Let's consider a case where only the amplitude is different in each of the axes.

- Transmissibility :  $T_x = 0.5$ ,  $T_y = 0.5$ ,  $T_z = 0.5$

- Amplitude of Vibration :  $|V^{b,M}| = [0.3 \quad 0.2 \quad 0.1]$

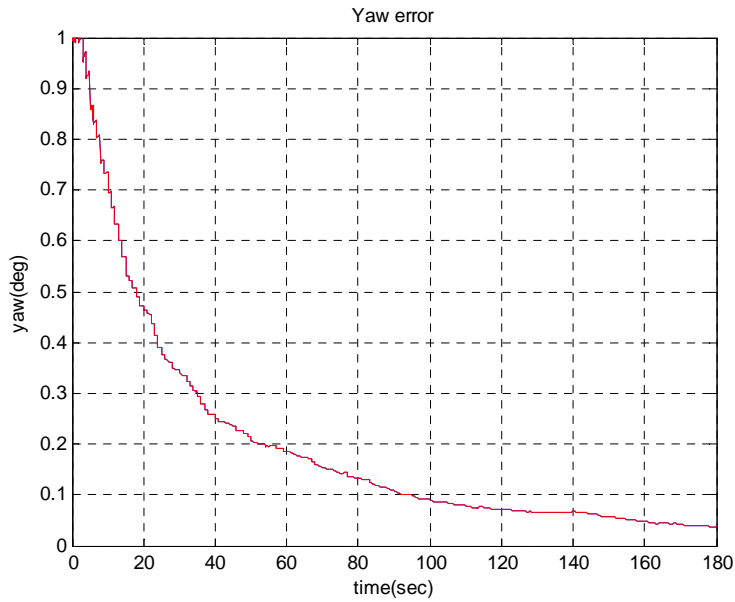


Figure 27. Yaw error result of the case with different amplitudes

The yaw error is properly estimated in this case. When only the amplitudes are different with other axes, transfer alignment will be possible.

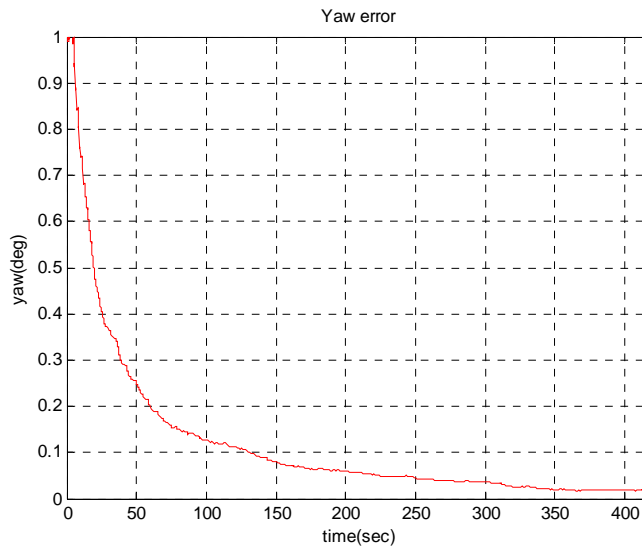


Figure 28. Yaw error result of transfer alignment for 7 minutes

If the alignment time is longer, the transfer alignment performance increase gradually. In the Figure 28, the result is the yaw error of the proposed transfer alignment method for 7 minutes. The yaw error converges gradually for whole simulation time.

In summary, if the proposed transfer alignment algorithm is used in the

following cases, better performance than conventional algorithm is expected.

1. The launcher is required to maintain a steady state.
2. The transmissibility of the vibration generated by the engine of the generator is measured in advance.
3. The Amplitude of the vibration is significantly different with each of the axes.



## **Chapter 4. Coning and Sculling Error Mitigation by Frequency Estimation**

Conventional coning and sculling mitigation methods are presented on Chapter. 2. The aforementioned algorithms use gyro outputs to calculate the higher-order correction terms. However, these algorithms have some performance limitations, because they assume that the signals are represented by polynomials. That is, the conventional polynomial representation of coning error does not faithfully express the sinusoidal oscillations. To resolve these drawbacks of conventional coning compensation algorithm, a new compensation method based on a signal processing technique. And we propose a direct compensation method based on a signal processing technique and show that the algorithm can also be applied to the sculling error as well. We employ an adaptive notch filtering algorithm to detect a sinusoidal signal from gyro measurements, and propose a method to accurately estimate the frequency, magnitude, and phase of the sinusoidal signal. From these parameters, we also derive higher-order compensation terms for the correction of coning/sculling errors.

## 4.1 Coning compensation

Angular rate vector in coning motion is expresses as Eq. (2.23).

$$\omega = \begin{bmatrix} a\Omega \cos \Omega \tau & b\Omega \cos(\Omega \tau + \varphi) & 0 \end{bmatrix} \quad (4.1)$$

By substituting into the equation (2.30), we can have

$$\delta\phi_m = \frac{1}{2} \int_{\tau_{m-1}}^{\tau_m} \alpha(\tau, \tau_{m-1}) \times \omega d\tau = \begin{bmatrix} 0 & 0 & (ab\Omega \sin(\varphi)/2) [T - (1/\Omega) \sin \Omega T] \end{bmatrix}^T \quad (4.2)$$

$\delta\phi_m$  means the theoretical coning error. This equation shows that the coning error term consists of the amplitudes of signal  $a, b$ , the frequency of signal  $\Omega$ , and phase difference  $\varphi$ .

A direct compensation method is proposed in this paper using these error characteristics. If we can estimate these parameters, then the exact coning compensation term can be computed using Eq. (4.2). Thus the signal estimation algorithm is utilized to estimate the exact coning compensation term. When sinusoidal signals occur in gyro during coning motion, signal estimation algorithm can detect sinusoidal signals. Then we can obtain

parameters to compensate the coning such as  $a, b$ ,  $\Omega$ , and  $\varphi$ . From these parameters, the exact coning compensation term can be calculated. Thus sinusoidal signal estimation is a key part of the new algorithm.

## 4.2 Sculling Compensation

Sculling motion is defined as sinusoidal angular motion on an axis and sinusoidal or linear acceleration motion on the body. In this case, the acceleration is defined as

$$\mathbf{f} = \begin{bmatrix} 0 & a \sin(\Omega t + \varphi) & 0 \end{bmatrix} \quad (4.3)$$

And the angular rate signal is

$$\omega_{ib}^b = \begin{bmatrix} \Omega b \cos \Omega t & 0 & 0 \end{bmatrix}^T \quad (4.4)$$

Then the sculling error is

$$\delta u_z^n = \frac{1}{2} ab \cos \varphi \int_{t_k}^{t_{k+1}} (1 - \cos \Omega(t - t_k)) dt \quad (4.5)$$

Evaluating the above integral,

$$\delta \ddot{u}_z^n = \frac{1}{2} ab \cos \varphi \left\{ 1 - \frac{\sin \Omega \delta t}{\Omega \delta t} \right\} \quad (4.6)$$

The same algorithm can be used for the sculling error compensation. If the amplitude of signal  $a$ ,  $b$ , the frequency of signal  $\Omega$ , and phase difference  $\varphi$  are estimated, the exact sculling compensation can be made.

### 4.3 Adaptive Notch Filtering for Signal Estimation

We used the adaptive notch filtering technique to estimate the parameters of the gyro signals. In signal processing, there are many techniques to extract a sinusoidal signal from a noisy original signal. Among these techniques, adaptive notch filtering has advantages such as a small time delay and accurate signal estimation performance. A notch filter is a kind of band stop filter that blocks signals only on a narrow frequency band, as shown in Figure. 29. This filter can be constructed by a transfer function with two zeros and two poles.

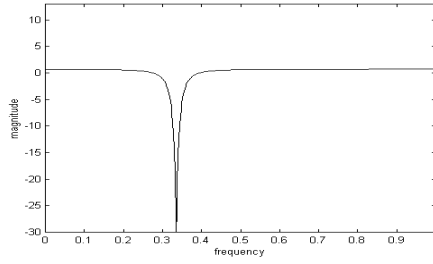


Figure 29. Frequency response of notch filter

The transfer function of the notch filter with the pole-zero pattern of Fig.27 can be represented as

$$H(z) = \frac{(1 - e^{j\omega_0} z^{-1})(1 - e^{-j\omega_0} z^{-1})}{(1 - \alpha e^{j\omega_0} z^{-1})(1 - \alpha e^{-j\omega_0} z^{-1})} \quad (4.7)$$

where  $\alpha$  is a parameter to adjust the bandwidth of notch filter, and  $\omega_0$  is the frequency of the sinusoidal signal of the gyro. The adaptive notch filter detects the sinusoidal component in the gyro signal by adapting its frequency.

The transfer function of the notch filter in Eq. (4.7) can also be written as

$$\begin{aligned} H(z) &= \frac{1 - 2\cos(\omega_0)z^{-1} + \alpha^2 z^{-2}}{1 - 2\alpha\cos(\omega_0)z^{-1} + \alpha^2 z^{-2}} \\ &= \frac{1 + 2k_0 z^{-1} + \alpha^2 z^{-2}}{1 + k_0(1 + \alpha')z^{-1} + \alpha^2 z^{-2}} \end{aligned} \quad (4.8)$$

where,  $k_0 = -\cos(\omega_0)$ . Hence, when the notch filter estimates adaptively, we can obtain the frequency of the signal  $\omega_0$ .

For a sinusoidal signal with unknown frequency, its frequency can be estimated online, by the adaptive notch filtering algorithm introduced in [72]:

$$\begin{aligned} D(n) &= \lambda D(n-1) + 2\varepsilon x(n-1)^2 \\ C(n) &= \lambda C(n-1) + \varepsilon x(n-1)^2 [x(n) + x(n-2)] \\ \hat{k}_0(n) &= \gamma \hat{k}_0(n-1) - (1-\gamma) \frac{C(n)}{D(n)} \end{aligned} \quad (4.9)$$

where  $\lambda$  and  $\varepsilon$  (which are related to  $\alpha$ ) are parameters to adjust the convergence rate of  $\hat{k}_0(n)$ , and  $\gamma$  is a parameter to mitigate the fluctuation of  $\hat{k}_0(n)$ .

Note that the notch filter removes the frequency component that corresponds to  $\hat{k}_0(n)$ , and hence if we subtract the output from the input, we can obtain the enhanced sine wave. From this we can estimate amplitude and phase difference of signal.

The performance of the proposed method can be degraded in the case that the oscillations are not steady, because there is some delay in tracking the varying frequency.

#### 4.4 Direct Coning/Sculling Compensation Algorithm

The proposed coning compensation algorithm works as shown in Figure 30.

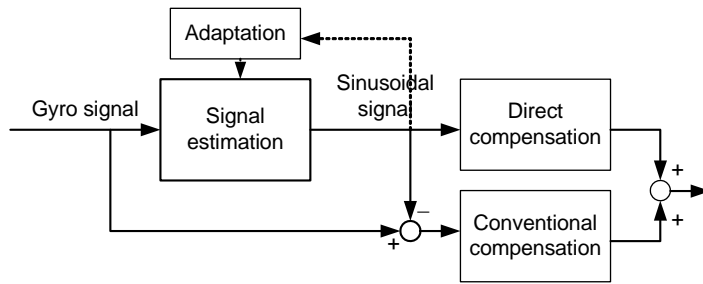


Figure 30. Attitude Compensation algorithm for pure coning motion

The algorithm is operated when a sinusoidal signal exists on gyro outputs. However, a non-commutativity error may appear not only on coning motion induced by a sinusoidal angular rate, but also on a general signal such as a linear angular rate signal. In this case, a conventional algorithm can eliminate the attitude error exactly.

Thus, the conventional algorithm and proposed algorithm must be used concurrently. Sinusoidal signals on gyro outputs, which generate coning errors, are extracted from the original signal and applied to the proposed direct coning compensation algorithm. The remainders are calculated by the

conventional algorithm. Using the proposed method, the rotation angle in Eq. (2.28) can be represented to Eq. (4.10) using proposed algorithm.

$$\phi = \alpha + \delta\phi_C + \delta\phi_D \quad (4.10)$$

Where  $\delta\phi_C$  and  $\delta\phi_D$  are the coning error correction terms. To be precise,  $\delta\phi_C$  is an attitude correction term that is calculated by conventional coning compensation algorithm, and  $\delta\phi_D$  is an attitude correction term calculated using the proposed coning compensation algorithm. If there are continuous oscillations in the vehicle, this signal estimation algorithm works appropriately, and the coning error can be mitigated exactly using the direct compensation method, whereas the conventional algorithms have some errors in this case.

On the other hand, if the oscillation signal does not exist, the conventional algorithm operates appropriately. In this case, the signal estimation algorithm does not work and  $\delta\phi_D$  will be zero. Then, the hybrid algorithm shows an identical result to conventional algorithm, and thus we can obtain proper results in both cases whether the oscillation exists or not.

The direct compensation method also has advantages over conventional methods in a noisy environment. Signal estimation uses a Least Square based



method that makes the algorithm robust to noisy signal. But in conventional method uses a signal sample directly, which may be influenced by signal noise.

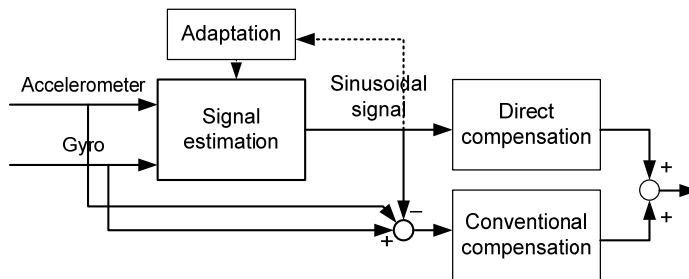


Figure 31. Velocity compensation algorithm for sculling motion

The sculling compensation algorithm is similar to coning algorithm. The signal estimation block extracts the sinusoidal components from accelerometer and gyro signal. Sinusoidal terms are used to compute the sculling compensation term. Sensor signal from which the sculling signal is removed, is used for conventional velocity computation.

## 4.6 Simulation results

Our first simulation result is a test for pure coning motion such as :

$$\omega_{ib}^b = \begin{bmatrix} a\Omega \cos \Omega \tau & b\Omega \cos(\Omega \tau + \varphi) & 0 \end{bmatrix}^T \quad (4.11)$$

Where,  $a = b = 1\text{rad}$ ,  $\Omega = 2\pi \times 30\text{Hz}$ ,  $\varphi = 90^\circ$  and sampling rate is  $100\text{Hz}$ .

Also, the gyro signals have noise of  $1\text{deg/hr}/\sqrt{\text{Hz}}$ , and bias of  $1\text{deg/hr}$ .

In this case, the gyro signal has only a sinusoidal component. The adaptive notch filter clearly converges within 10 samples. Thus, the proposed coning compensation method works well.

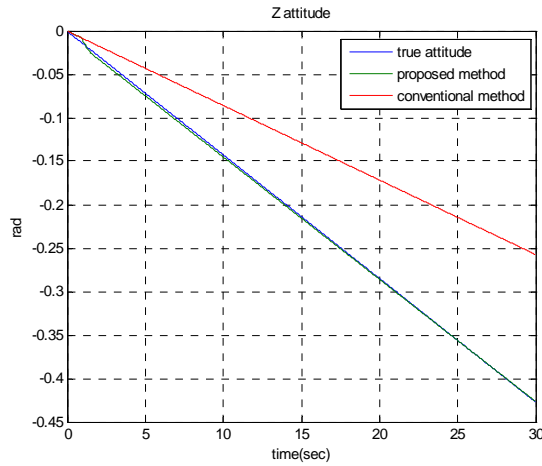


Figure 32. Attitude result for pure coning motion

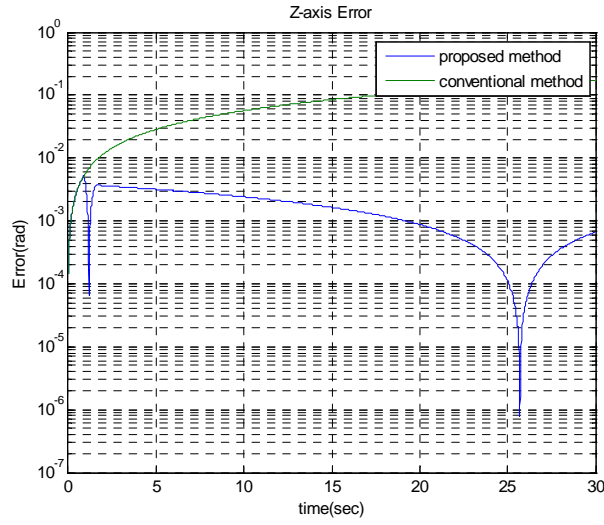


Figure 33. Attitude error for pure coning motion

In Fig. 32, the blue line is the true attitude and the red line is the result of the conventional method. The conventional method uses Miller's "one sample plus one previous per update" algorithm. The conventional algorithm is expressed as:

$$\delta\phi_c = \frac{1}{12} \omega(k-1) \times \omega(k-1) \times dt^2 \quad (4.12)$$

The conventional algorithm has theoretical error is

$$\alpha_\varepsilon = \frac{ab}{60}(\Omega dt)^5 \quad (4.13)$$

The result of the proposed algorithm (green line) shows better performance than the result of the conventional method. Both algorithms show the same result in the first 0.5 s, which means that the adaptive notch filter had not converged in 0.5 s, and only conventional algorithm worked. When the adaptive notch filter parameter estimation converges around from 0.5s, direct compensation corrected the coning compensation term almost exactly.

Therefore, the proposed method shows at least the performance of the conventional method.

Figure 33 shows the attitude error on a log scale. The results of the proposed algorithm show much better performance over all time increments.

The next simulation is smaller coning error case. Because the error of conventional algorithm (1sample and 1previous sample algorithm) yields

$$\frac{ab}{60}(\Omega dT)^5, \text{ lower frequency coning motion makes smaller coning error.}$$

$a = b = 1\text{rad}$ ,  $\Omega = 2\pi \times 10\text{Hz}$ ,  $\varphi = 90^\circ$  is used in this simulation.

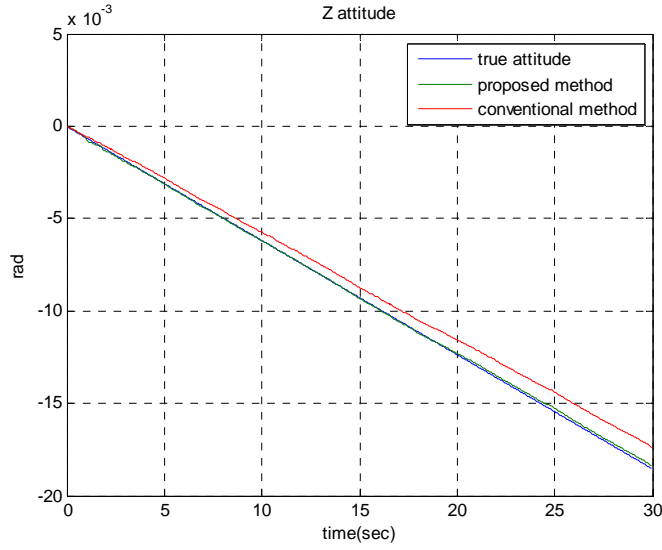


Figure 34. Result of 10Hz coning motion

In this result, coning error decreased to  $10^{-2}$  radian level for 30 seconds. The proposed algorithm shows better result than conventional algorithm, however, performance gap is narrowed. Thus, the proposed algorithm is more powerful on large coning error by high frequency coning motion.

The next simulation result shows performance of adaptive notch filter for changing coning motion. In this case, the coning signal with  $a = b = 1\text{rad}$ ,  $\Omega = 30\text{Hz}$ , and  $\varphi = 90^\circ$  exists for only 0~10 s, 15~20 s, and 25~30 s. The simulation result of three-time coning motion shows the parameter estimation filtering performance for a more dynamic situation.

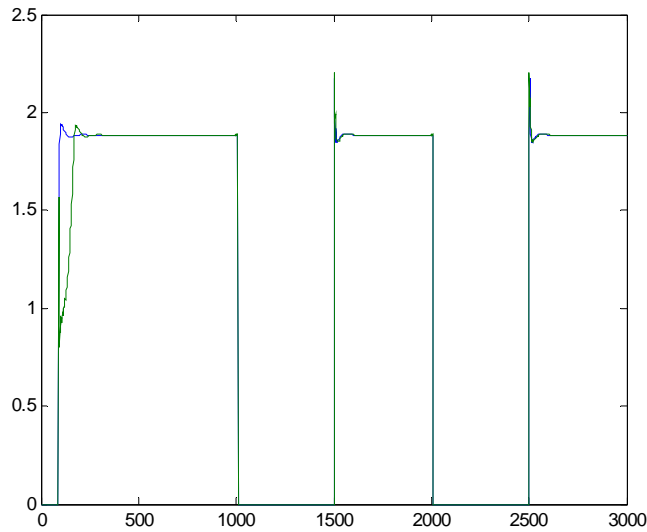


Figure 35. Frequency estimation result (green : x-axis, blue : y-axis)

Figure 35 shows the frequency estimation result of adaptive notch filter. The adaptive notch filter converged quickly, within at least 0.5 s. Frequency estimation converged on the second and third coning motion more quickly than on the first coning motion. For the first motion, the filter needs some samples to converge due to the nature of adaptive algorithm. However, our proposed algorithm demonstrates better performance over the conventional algorithm for all times increments, as shown in Figure 36.

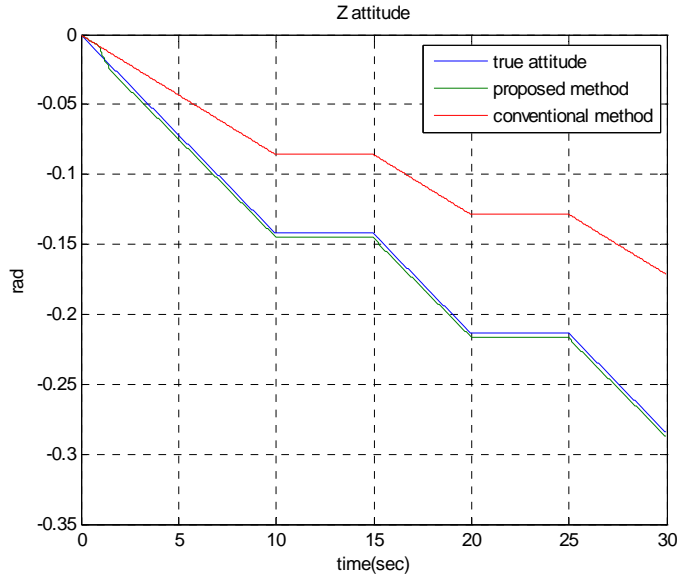


Figure 36. Attitude result for changing coning motion

Whenever the filter does not estimate the parameters correctly, the proposed coning compensation algorithm acts the same as the conventional algorithm. This guarantees the robustness of the proposed algorithm.

Next simulation is the result of coning motion with angular rate. The signal in this case is expressed as:

$$\omega_{ib}^b = \begin{bmatrix} at + a\Omega \cos \Omega \tau & bt + c + b\Omega \cos(\Omega \tau + \varphi) & 0 \end{bmatrix} \quad (4.12)$$

This signal is composed of linear angular rate angular rate component and coning signal. The linear angular component, which is combined with sinusoidal component of the other axis, can make a little attitude error but it is

not negligible.

The result for this case is shown in Fig. 37.

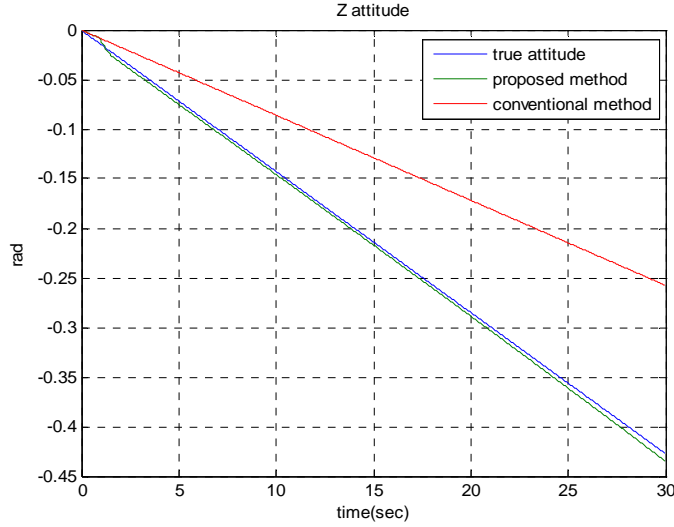


Figure 37. Attitude result for Coning motion & general linear angular rate

In this case, the result shows a similar trend to pure coning case. The direct compensation algorithm treats the coning error component effectively, and the rest of errors induced by linear component are compensated by conventional compensation block. Conventional algorithm can remove the attitude error induced by linear component.

Another reason for this trend is that the coning error is dominant attitude error source, and the attitude error induced by linear terms is relatively small.



It cannot be displayed too large to be separated from coning error.

The next simulation is sculling test. The sculling motion is defined as Eq. (2.36). The parameters of sculling motion are  $a=5g$  ,  $f=10Hz$  , and  $b=1rad$  . Then the velocity computation result of D direction is shown in Fig. 38.

The blue line is the true attitude and the red line is the result of the conventional method. In this case, X Y axis oscillations make the Z axis velocity error. The conventional method uses Miller's "one sample plus one previous per update" algorithm. The proposed algorithm shows better result than conventional algorithm.

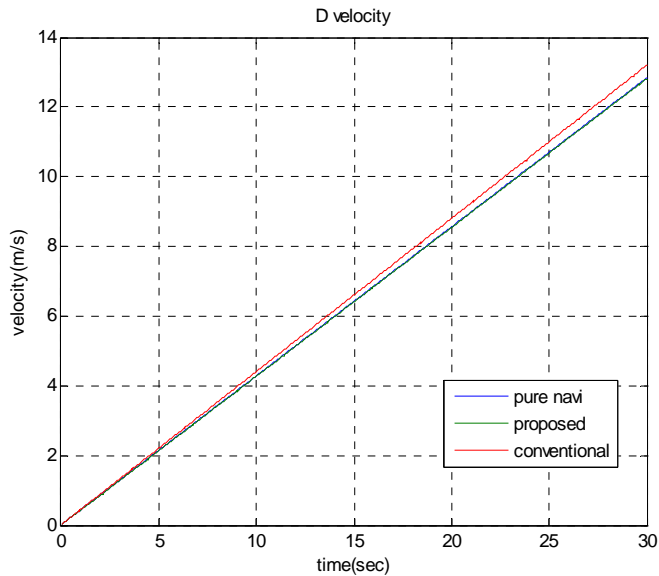


Figure 38. Velocity result for pure sculling motion

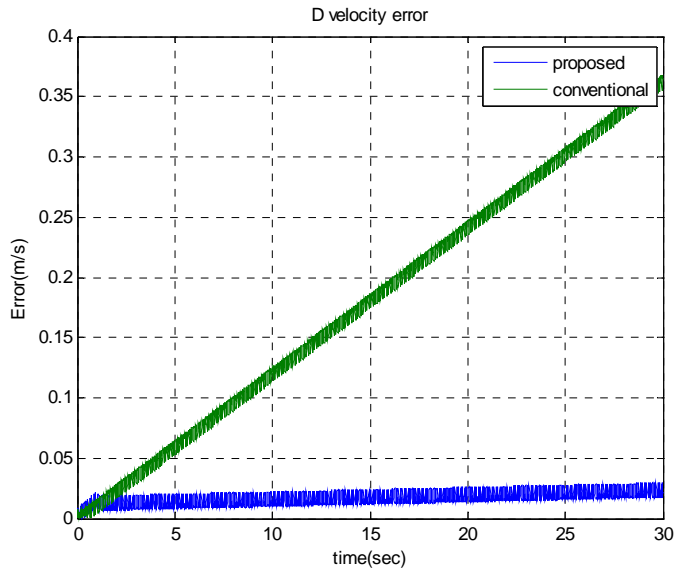


Figure 39. Velocity error of D direction for pure sculling motion

Fig. 39 shows the velocity error. Conventional algorithm has error which rapidly increases with time. On the other hand, the proposed algorithm shows less error. The result of proposed algorithm before 0.5 sec is bad because the signal estimation filter did not converge.

In order to verify for the real sensor, rate table test is conducted

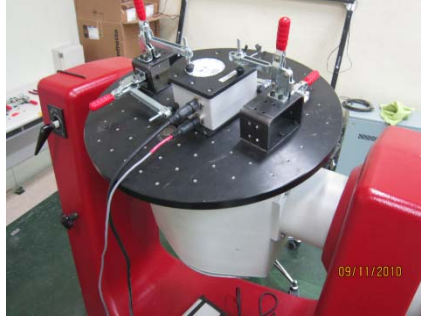


Figure 40. Rate table test with HG1700

The rate table used for a test is ACT2000 Model 246 of Acutronics Inc. and the IMU is HG1700, which has 1deg/hr gyro bias and made by Honeywell Inc..

To make the coning motion, the rate table rotated with oscillatory motion. The parameters of coning motion made by the rate table are  $a=b=10^\circ$ ,  $\Omega=1\text{Hz}$ ,  $\varphi=173^\circ$  and the sampling rate is 100Hz. Then, the theoretical coning error for 20sec is

$$\delta\phi_m = (a_i b_i \Omega_i \sin(\phi_i) / 2) [T - (1 / \Omega_i) \sin \Omega_i T] \approx 13.12 \text{ deg} \quad (4.12)$$

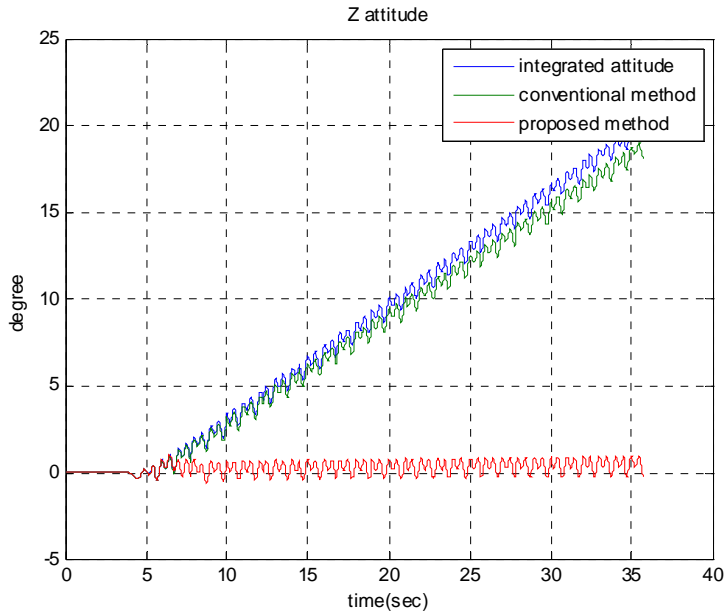


Figure 41. Attitude result of rate table coning motion

Then the attitude computation result of Z direction is shown in Fig. 41. The rate table was started at 5 second. The blue line is the integrated attitude without any coning mitigation method, and the green line is the result of the conventional method which uses Miller's "one sample plus one previous per update" algorithm [24]. The red line represents the result of the proposed direct compensation method. The magnitude of coning error occurs about 13 degrees for 20 seconds after the rotation begins. It is the similar value of theoretical coning error estimated. In this test, the phase differences are 173 degrees, not 90 degrees. Thus the conventional method, which assumes the

phase difference of each axis on coning error as 90 degrees, cannot properly mitigate the coning error. However, as new proposed algorithm estimates the phase differences of coning signal, new method can mitigate the coning error regardless of phase differences. Therefore the proposed algorithm outperforms conventional algorithm. It mitigates the error below 1degree level in 30 seconds.

## Chapter 5. Conclusion

In this dissertation, performance improvement methods applying frequency domain approaches to inertial navigation system are discussed. The conventional INS algorithm computes all navigation solutions in the time domain. There are some problems which are impossible to resolve only by computation in the time domain. Thus, frequency domain approaches are applied to resolve the observability problem of the transfer alignment and the coning/sculling error mitigation algorithm.

The first topic is the transfer alignment method. The typical transfer alignment estimates the initial attitude and velocity of SINS using INS result of MINS as measurements. The typical method shows a low accuracy in a steady-state launcher due to the lack of observability. Thus, a new transfer alignment algorithm that uses a frequency domain technique is proposed in order to solve the observability problem. When vibrations of the engine of a ground vehicles exist, the same vibration can be measured by MINS and SINS with different effects. The attitude difference between MINS and SINS can be estimated using different measured amplitudes. Using the vibration of the vehicle in a stationary state, the amplitude measurements are used to estimate the yaw angle of the stationary vehicle. As a result, the misalignment angle is

properly estimated by using a Kalman filter that takes into account the new amplitude measurement. The simulation results also confirm that the filter makes the yaw angle observable. However, there are some drawbacks to using only the amplitude measurements. At first, the proposed algorithm requires two different sources of vibration. The second problem is that the proposed method assumes the connector between launcher and projectile is a rigid body, and the third problem is that roll and pitch estimation performance of the proposed method are degraded relative to the conventional method. The final problem is that the proposed algorithm can estimate only misalignment angles.

Thus the amplitude measurement-augmented transfer alignment algorithm was developed by integrating amplitude measurements to a conventional transfer alignment filter, and transmissibility is considered in the measurement model. As a result, yaw estimation performance is improved with only one vibration signal. The proposed transfer alignment method can be used for rapid transfer alignment on stationary ground vehicles, and this work shows the possibility of new measurements for alignment.

The third topic is coning/sculling error compensation algorithm. Typical coning and sculling compensation algorithms are conducted by using the cross product between inertial sensor measurements. These methods have limitations with respect to the performance on the vibrating body. A new

algorithm is proposed algorithm with a direct coning/sculling compensation method. Our new method uses adaptive notch filtering that estimates the parameters in sinusoidal signals on gyro outputs, thus providing more precise compensation. If there are continuous sinusoidal signals on the gyros, an adaptive notch filter can be used to estimate the parameters of the sinusoidal signals, and a the direct coning/sculling compensation algorithm computes the attitude correction term produced by the coning/sculling signal. Our simulation results show that the proposed algorithm can be used in the vehicle with a high frequency of coning and sculling motion.



## References

- [1] <http://www.britannica.com/EBchecked/topic/407011/navigation>
- [2] G. T. Schmidt, "INS/GPS Technology Trends," RTO Educational Notes, RTO-EN-SET-064, 2004.
- [3] D. H. Titterton, J.L. Weston, *Strapdown Inertial Navigation Technology*, Peter Peregrinus Ltd, 1997.
- [4] Paul D. Groves, *Principles of GNSS, inertial, and multisensor integrated navigation systems*. Artech House, 2013.
- [5] Oleg Stepanovich Salychev, *Applied Inertial Navigation: problems and solutions*. Moscow, BMSTU Press, 2004.
- [6] Esmat Bekir, *Introduction to modern navigation systems*. NJ, USA, World Scientific, 2007.
- [7] G. M. Siouris, *Aerospace Avionics Systems : A Modern Synthesis*, Academic Press, Inc., 1993.
- [8] B. H. Browne, and D. H. Lackowski. "Estimation of dynamic alignment errors in shipboard fire control systems." IEEE Conference on Decision and Control including the 15th Symposium on Adaptive Processes. Vol. 15. IEEE, 1976.
- [9] J. Kain, J. Cloutier, "Rapid transfer alignment for tactical weapon applications," AIAA Guidance, Navigation and. Control Conference,

1989.

- [10] D. Tarrant, C. Roberts, D. Jones, C. Yang, C. F. Lin, "Rapid and robust transfer alignment. In Aerospace Control Systems,". Proceedings. The First IEEE Regional Conference on, pp. 758-762, 1993.
- [11] D. H. Titterton, J. L. Weston, "The alignment of ship launched missile IN systems," In Inertial Navigation Sensor Development, IEE Colloquium on, IET, 1990.
- [12] Paul D. Groves, Genevieve G. Wilson, Christopher J. Mather. "Robust rapid transfer alignment with an INS/GPS reference." Proceedings of the 2002 National Technical Meeting of The Institute of Navigation, 2001.
- [13] You-Chol Lim, Lyou Joon, "An error compensation method for transfer alignment." Electrical and Electronic Technology, 2001. TENCON. Proceedings of IEEE Region 10 International Conference on. Vol. 2. IEEE, 2001.
- [14] Changyue Sun, and Deng Zhenglong. "Transfer alignment of shipborne inertial-guided weapon systems." Journal of Systems Engineering and Electronics, Vol.20, No.2, pp. 348-353. 2009.
- [15] Xiaorong, Shen, and Shi Yongzhu. "Angular rate matching method

- for shipboard transfer alignment based on  $H^\infty$  filter." 6th IEEE Conference on Industrial Electronics and Applications (ICIEA), 2011.
- [16] Jingshuo Xu, Yongjun Wang, and Zhicai Xiao. "Rapid transfer alignment for SINS of carrier craft." *Journal of Systems Engineering and Electronics*, Vol. 24, No. 2. pp. 303-308, 2013.
- [17] Groves, Paul D. "Optimising the transfer alignment of weapon INS." *Journal of Navigation* Vol. 56, No. 2, pp. 323-335, 2003.
- [18] P. G. Savage, "Strapdown Inertial Navigation Algorithm Design Part I: Attitude Algorithms," *Journal of Guidance, Control, and Dynamics*, Vol. 21, No. 1, 1998, pp. 19-28.
- [19] P. G. Savage, "Strapdown Inertial Navigation Algorithm Design Part II: Velocity and Position Algorithms," *Journal of Guidance, Control, and Dynamics*, Vol. 21, No. 1, 1998, pp. 19-28.
- [20] G. J. Kim, C. G. Park, M. J. Yu, "Noncommutativity Error Analysis with RLG-based INS," *Journal of KSAS*, Vol. 34, No. 1, 2006.
- [21] G. J. Kim, T. G. Lee, "Analysis of the two-frequency coning motion with SDINS," *AIAA Guidance, Navigation, and Control Conference*, Montreal, Canada, 2001.
- [22] K. M. Roscoe, "Equivalency Between Strapdown Inertial

- Navigation Coning and Sculling Integrals/Algorithms,” Journal of Guidance, Control and Dynamics, Vol. 24, No. 2, 2001.
- [23] J. E. Bortz, "A New Material Formulation for Strapdown Inertial Navigation," IEEE Trans. Aerospace and Electronic Systems, Vol. 7, No. 1, 1971.
- [24] R. B. Miller, "A New Strapdown Attitude Algorithm," Journal of Guidance, Control and Dynamics, Vol. 6, No. 4, 1983.
- [25] M. B. Ignagni, "Optimal Strapdown Attitude Integration Algorithms," Journal of Guidance, Control and Dynamics, Vol. 13, No. 2, 1990.
- [26] M. B. Ignagni, "Efficient Class of Optimal Coning Compensation Algorithms,” Journal of Guidance, Control, and Dynamics, Vol. 19, No. 2, 1996.
- [27] Y. F. Jiang, and Y. P. Lin, "On the Rotation Vector Differential Equation,” IEEE Transactions on Aerospace and Electronic Systems, Vol. AES- 27, No. 1, 1991.
- [28] Y. F. Jiang, and Y. P. Lin, "Improved Strapdown Coning Algorithms,” IEEE Transactions on Aerospace and Electronic Systems, Vol. AES- 28, No. 2, 1992.
- [29] J. G. Lee, Y. J. Yoon, J. G. Mark, and D. A. Tazartes, "Extension

- of Strapdown Attitude Algorithm for High-Frequency Base Motion,”  
Journal of Guidance, Control, and Dynamics, Vol. 13, No. 4, 1990.
- [30] J.G. Mark and D.A. Tazartes., “Application of coning algorithms to  
frequency shaped gyro data,” Saint Petersburg International  
Conference on Integrated Navigation Systems, 6th, St. Petersburg,  
Russia, 1999.
- [31] C. G. Park, K. J .Kim, J. G. Lee, D. Chung, "Formalized Approach  
to Obtaining Optimal Coefficients for Coning Algorithms," Journal  
of Guidance, Control, and Dynamics, Vol. 22, No.1, 1999.
- [32] Chul Woo Kang, C. G. Park, N. I. Cho, "New Coning Error  
Compensation Method Using Direct Signal Estimation," 18th IFAC  
Symposium on Automatic Control in Aerospace, Japan, 2010.
- [33] Chul Woo Kang, N. I. Cho, C. G. Park. "Approach to direct  
coning/sculling error compensation based on the sinusoidal  
modelling of IMU signal." IET Radar, Sonar & Navigation Vol. 7,  
No. 5, pp. 527-534, 2013.
- [34] Mohinder S. Grewal, Lawrence R. Weill, and Angus P. Andrews.  
Global positioning systems, inertial *navigation, and integration*.  
John Wiley & Sons, 2007.
- [35] Guowei Cai, Ben M. Chen, and Tong Heng Lee, *Unmanned*

*rotorcraft systems*, Springer, 2011.

- [36] Van Der Ha, Jozef C., and Malcolm D. Shuster. "A tutorial on vectors and attitude [Focus on Education]." *Control Systems*, IEEE Vol. 29, No. 2, pp. 94-107, 2009.
- [37] Malcolm D. Shuster, and F. Landis Markley. "Generalization of the Euler angles." *Journal of the Astronautical Sciences*, Vol. 51, No. 2, 123-132, 2003.
- [38] Arend L. Schwab, "Quaternions, finite rotation and euler parameters." *Articulo publicado en su propia página web*, 2002.
- [39] C. G. Park, K. J. Kim, H. W. Park and J. G. Lee, "Development of an Initial Coarse Alignment Algorithm for Strapdown Inertial Navigation System," *Journal of Control, Automatic, and Systems*, Vol. 4, No. 5, pp.674-679, 1998.
- [40] Kwangjin Kim, "INS/GPS integration system based on the unscented kalman filter," *Ph. D. dissertation*, Seoul National University, Seoul, 2008.
- [41] I. Y. Bar-Itzhack and N. Berman, "Control Theoretic Approach to Inertial Navigation Systems," *Journal of Guidance*, Vol. 11, No. 3, 1988
- [42] C. G. Park, K. J. Kim, H. W. Park and J. G. Lee, "Development of

- an Initial Coarse Alignment Algorithm for Strapdown Inertial Navigation System,” Journal of Control, Automatic, and Systems, Vol. 4, No. 5, pp.674-679, 1998.
- [43] Y. F. Jiang and Y. P. Lin, "Error Estimation of INS Ground Alignment Through Observability Analysis," IEEE Transactions on Aerospace and Electronic Systems, Vol. 28, No. 1, 1992
- [44] Andrey Soloviev and Frank van Graas, “Enhancement of Integrated GPS/INS Performance Utilizing Frequency Domain Implementation of INS Calibration,” NAVIGATION, Journal of the Institute of Navigation, Volume 54, Number 2, 2007.
- [45] Goshen-Meskin, D., Bar-Itzhack, I.Y., "Observability analysis of piece-wise constant systems. I. Theory," Aerospace and Electronic Systems, IEEE Transactions on , vol.28, no.4, pp.1056-1067, Oct 1992.
- [46] Y. M. Yoo, J. G. Park, D. H. Lee, and C. G. Park, "A Theoretical Approach to Observability Analysis of the SDINS/GPS in Maneuvering with Horizontal Constant Velocity," International Journal of Control, Automation, and Systems, Vol.10, No.2, pp.298-307, April 2012.
- [47] Oppenheim, Alan V., Ronald W. Schafer, and John R. Buck.

Discrete-time signal processing. Vol. 5. Upper Saddle River:  
Prentice Hall, 1999.



## 초 록

본 논문에서는 관성항법시스템에 대해 새로운 주파수 영역에서의 접근을 통해 기존 시스템에서 해결할 수 없는 문제들을 해결하는 연구를 수행하였다.

관성항법 알고리즘은 1950년대 처음 개발되기 시작하여 현재 다양한 자동제어 분야에 적용되고 있다. 그러나 관성항법 알고리즘의 주요 알고리즘들은 모두 시간 영역에서 연산을 수행하기 때문에 전달정렬에서의 가관측성 문제나 코닝/스컬링 오차와 같이 해결이 불가능한 문제들이 발생한다.

본 논문에서는 기존 관성항법 알고리즘에 대한 주파수 영역의 신호 분석을 통한 새로운 접근 방식을 통해 기존 방식으로는 해결할 수 없는 문제를 해결하는 방법을 제안하였다. 우선 새로운 형태의 전달 정렬 알고리즘을 제안하였다. 기존 전달정렬 기법은 칼만필터를 이용한 속도/자세 정합 방식을 사용한다. 이러한 방식을 사용하는 경우, 가관측성 문제로 인해 정렬 성능은 발사대의 기동에 의해 결정된다. 특히 정지상태에서의 정렬은 가관측성의 부족으로 인하여 매우 긴 시간을 요구하게 된다. 그러나 본 논문에서는 차량의 엔진 등에서 발생하는 진동의

특성을 이용, 새로운 벡터 측정치를 제안함으로써 가관측성 문제를 해결하였다. 시뮬레이션을 통하여 새로 제안된 알고리즘은 정지상태에서도 빠르게 정렬을 수행할 수 있음을 보이고 있다.

또한 주파수 영역의 관점에서 코닝/스컬링 오차 감소 기법에 대한 연구도 수행되었다. 기존 코닝/스컬링 오차 감소 기법은 신호의 단순 연산에 의해 이루어 졌으며 이론적으로 보상할 수 없는 오차가 존재한다. 그러나 본 논문에서 제안된 코닝/스컬링 오차 감소 기법은 적응 노치필터를 이용하여 오차를 정확하게 추정하여 이를 제거하는 방식을 사용하므로 일정한 진동에 의한 코닝/스컬링 오차를 기존 기법에 비하여 크게 감소시킬 수 있음을 보인다.

주요어: 관성항법시스템, 칼만 필터, 전달정렬 기법, 복합항법 시스템,  
코닝/스컬링 오차

이 름: 강 철 우

학 번: 2007-20756